Speciation of organic aerosols in the Saharan Air Layer and in the free troposphere westerlies

M. Isabel García[1,2], Barend L. van Drooge[3], Sergio Rodríguez[1] and Andrés Alastuey[3]

[1] Izaña Atmospheric Research Centre, AEMET, Joint Research Unit to CSIC "Studies on Atmospheric Pollution", Santa Cruz de Tenerife, 38001, Spain
[2] Department of Chemistry (T.U. Analytical Chemistry), Faculty of Science, University of La Laguna, La Laguna, 38206, Spain
[3] Institute of Environmental Assessment and Water Research, CSIC, Barcelona, 08034, Spain

Correspondence to: Sergio Rodríguez (srodriguezg@aemet.es)

Abstract. We focused this research on the composition of the organic aerosols transported in the two main airflows of the subtropical North Atlantic free troposphere: (i) the Saharan Air Layer – the warm, dry and dusty airstream that expands from North Africa to the Americas at subtropical and tropical latitudes – and (ii) the westerlies – which flows from North America through the North Atlantic at mid and subtropical latitudes –. We determined the inorganic compounds (secondary inorganic species and elemental composition), elemental carbon and the organic fraction (bulk organic carbon and organic speciation) present in the aerosol collected at Izaña Observatory, ~2400 m a.s.l.. in Tenerife Island. The concentrations of all inorganic and almost all organic compounds were higher in the Saharan Air Layer than in the westerlies, with bulk organic matter concentrations within the range 0.02–4.0 $\mu g \cdot m^{-3}$. In the Saharan Air Layer, the total aerosol population was by far dominated by dust (93% of bulk mass), which was mixed with secondary inorganic pollutants (<5%) and organic matter (~1.5%). The chemical speciation of the organic aerosols (levoglucosan, dicarboxylic acids, saccharides, n-alkanes, hopanes, polycyclic aromatic hydrocarbons and those formed after oxidation of α-pinene and isoprene, determined by gas-chromatography coupled to mass-spectrometry) accounted for a 15% of the bulk organic matter (determined by the thermo-optical transmission technique); the most abundant organic compounds were saccharides (associated with surface soils), secondary organic aerosols linked to oxidation of biogenic isoprene (SOA ISO) and dicarboxylic acids (linked to several primary sources and SOA). When the Saharan Air Layer shifted southward, Izaña was within the westerlies stream and the organic matter accounted for ~28% of bulk mass of the aerosol cocktail. In the westerlies, the determined organic aerosol species accounted for 64% of the bulk organic matter, being SOA ISO and dicarboxylic acids the most abundant; the highest concentration of organic matter (3.6 $\mu g \cdot m^{-3}$) and of some organic species (e.g. levoglucosan and some dicarboxylic acids) were associated with biomass burning linked to a fire in North America. In the Saharan Air Layer, the correlation found between SOA ISO and nitrate suggests a large-scale impact of the enhancement in the formation of secondary organic aerosols due to interaction with anthropogenic NO_x emissions.

1 Introduction

Atmospheric aerosols, or particulate matter, influence on processes affecting climate, on continental and marine ecosystems, and on human health. The magnitude of these effects depends on the aerosols composition, which may include secondary inorganic species (e.g. sulphate, nitrate, ammonium and sea salt), mineral dust, elemental carbon and a number organic species constituting the so-called organic aerosols (OA) (IPCC, 2013). OA account for an important fraction of particulate matter, ranging from ~20% (continental mid-latitudes) to ~90% (tropical forested areas) (Kanakidou et al., 2005). As other aerosol components, OA also contributes to (i) light scattering and absorption (Kirchstetter and Novakov, 2004), (ii) cloud formation providing cloud condensation and ice nuclei (Sun and Ariya, 2005), and (iii) heterogeneous chemical reactions in the atmosphere (Kanakidou et al., 2005).

Principal sources of Primary OA (POA) include vegetation, fossil fuel combustion, biomass burning, biological aerosols and particles from soils. Precursors of Secondary OA (SOA) include natural and anthropogenic sources (Volkamer, et al., 2006; Gouw and Jimenez, 2009); emissions of biogenic volatile organic compounds (VOCs) significantly contribute to the global budget of SOA (Guenter et al., 2012). Some important factors influencing SOA formation are reactive nitrogen species (NO_x) (Presto et al., 2005; Ng et al., 2007, 2008), which are further oxidized to the highly reactive nitrate radical (NO_3). NO_3 interacts with VOCs in gas-phase, likely having an impact in global OA levels as indicated by modelling (Pye et al., 2010) and experimental work (Surratt et al., 2006). At daytime, NO_x can react with organic peroxy radicals (RO_2) resulting in peroxy nitrates (RO_2NO_2) and alkyl and multifunctional nitrates ($RONO_2$) (O'Brien et al., 1995); the formation of organic nitrates provisionally sequesters NO_x, which can suffers long-range transport to more remote environments (Horowitz et al., 1998; Mao et al., 2013). At nighttime, the interaction VOCs-NO_3 dominates, with SOA yields greater than that for OH or O_3 oxidation (Ng et al., 2017 and references there in). Previous modeling studies carried by Hoyle et al. (2007) suggested that, during twilight conditions, ~ 21% of the global average SOA may be due to oxidation of SOA precursors by NO_3, and measurements performed by Brown et al. (2009) found that, during nighttime, 1-17% of SOA was the result of NO3 initiated isoprene oxidation. In remote environments, VOCs enhance condensational growth of new particles which can enter to the free troposphere (FT) by means of elevated mounts (García et al., 2014). These tropospheric aerosols are subject to much greater lifetimes and wind speed than in the planetary boundary layer (BL), favouring long-range atmospheric transport and aerosol impacts (Winker et al., 2013). The aged and processed long-range transported OA is of particular interest, as is spatially representative of the remote background conditions having important implications for global air quality and climate.

The most extended technique to quantify the amount of bulk organic and elemental carbon in the atmospheric aerosols is the thermo-oxidant combustion and optical detection (Birch and Cary, 1996; Cavalli et al., 2010; Karanasiou et al., 2015). This is a useful method for mass closure, but does not provide information on OA speciation and consequently on OA sources and properties related to impacts. Alternatively, gas-chromatography coupled to mass-spectrometry analysis of aerosol samples allows the speciation of the organic compounds and the quantification of many of those identified as tracers for distinguish

sources and processes contributing to the budget of OA (Bauer et al. 2008; Mazurek et al. 1989; Claeys et al., 2007; Hallquist et al., 2009; Howsam and Jones 1998; Iinuma et al., 2007; Kawamura and Kaplan, 1987; Medeiros and Simoneit 2007; Narukawa et al., 1999; Rogge et al., 1993; Shauer et al. 2002; Simoneit et al. 1991; Simoneit et al. 2004a; Simoneit, 2002; Szmigielski et al., 2007). A number of studies have focused on OA speciation in urban areas (Alier et al., 2013; Kawamura and Kaplan, 1987; Puxbaum et al., 2007; Schauer et al., 1996; Simoneit et al., 1991; Van Drooge and Grimald, 2015) compared to remote environments. Studies in the free troposphere are scarce (Simoneit et al. 2004b; Fu et al., 2008, 2014; Wang et al., 2009; van Drooge et al., 2010; Meng et al., 2014), even if they are of interest due to the long-range transport potential linked to the high wind speeds above the boundary layer.

In this study we focused on the OA transported from inner Sahara over the North Atlantic in the so-called Saharan Air Layer (SAL; Prospero and Carlson, 1972). In summertime, the continental BL depth grows up to 5 km a.s.l. over the Sahara (Cuesta et al., 2009) and the prevailing easterly winds prompt the export of the warm Saharan air to the North Atlantic above the cool NNE trade winds that blows in the marine boundary layer. This results in the development of the SAL – a warm, dry and stable air stream that expands from North African coast, at altitudes 2 to 5 km a.s.l., to the Americas (Prospero and Carlson, 1972; Tsamalis et al., 2013) –. Because of the high stability associated with the warm air above the cool marine air, the SAL acts as a band conveyor that transport continental Saharan dusty air – originally placed near ground – over the North Atlantic; in addition to dust, other substances such as pollutants, vegetation debris or microorganisms are carried mixed with dust.

OA in the SAL has received little attention, even if its impacts are of interest. Anthropogenic bioaccumulative and toxic organic compounds (including organochlorine and organophosphate pesticides, polycyclic aromatic hydrocarbons, polychlorinated biphenyl) are transported from Western Sahara to the Caribbean within the SAL (Garrison et al., 2013). Viruses, bacteria, fungal and pollens also travels mixed with dust across the Atlantic (Griffin et al., 2007; Izquierdo et al., 2011). Field measurements in the SAL at Izaña Observatory found dust being the major ice nuclei at temperatures colder than -30ºC (Boose et al., 2016), whereas the observed ice nuclei at -8ºC points to a role of OA as ice nuclei at warm temperatures (Conen et al., 2015).

In this study we primarily focused on the origin of OA in the SAL. We collected in-situ aerosol samples directly into the high-altitude SAL at Izaña Observatory, located at ~2400 m a.s.l. in Tenerife Island. The profile of the organic species was used for a source apportionment of the bulk organic matter. The results were compared with a similar data set obtained during the same campaign under the westerlies (WES) airflow that regularly brings air from North America across the North Atlantic. The observed differences illustrate the diversity of OA sources over the North Atlantic free troposphere.

2 Methodology

2.1 Sampling site

Sample collection was performed at the Izaña Global Atmospheric Watch (GAW) Observatory in Tenerife island (Fig. 1; 16º29'58"W, 28º18'32"N). The site is located on a mountaintop (2373 m a.s.l), surrounded by a pine forest (limited between ~500–2300 m). The Observatory remains almost permanently above the temperature inversion layer associated to the trade winds, which separates the moist marine BL from the dry FT avoiding vertical mixing before sunrise. Sunlight during daytime activate thermal convection, developing an orographic thermal-buoyant upslope winds, that transport species emitted in the BL by biogenic and anthropogenic sources (see details in Rodríguez et al., 2009).

2.2 Sampling

Samples were collected within the annual aerosols summer campaign of the Izaña Observatory in August 2013. Particulate Matter (PM) was collected on pre-heated (at 205ºC) quartz filters (Pall Science 150 mm diameter) on high volume air samplers (Hi-Vol; MCZ) at a flow rate of 30 $m^3 \cdot h^{-1}$. 30 samples of total particulate matter (PM_T) were collected daily during nighttime (22:00–6:00 GMT; FT) and 12 samples of particulate matter smaller than 2.5 µm ($PM_{2.5}$) in non-consecutive days during daytime (10:00–16:00 GMT; BL). Field blanks were collected weekly and treated like the samples regarding preparation, transport and storage, as part of the quality assurance / quality control (QA/QC) protocol.

2.3 Chemical Analysis

2.3.1 Organics

One quarter of the filter sample was used for the organic compounds speciation by gas-chromatography coupled to mass-spectrometry (GC-MS). A detailed description of the analytical method is given elsewhere (Fontal et al. 2015, van Drooge and Grimalt 2015). Briefly, filters were spiked with deuterated standards of acids, anhydro-saccharides, alkanes, and polycyclic aromatic hydrocarbons (PAHs), and extracted ultrasonically in a mixture of dichloromethane and methanol. Extracts were filtered and concentrated until 0.5 mL. For the analysis of polar compounds, i,e. acids and saccharides, a 25 µL aliquot of the extract was evaporated until dryness, and 25 µL of bis-(trimethylsilyl)-trifluoroacetamide (BSFTA) + trimethylchlorosilane (99:1) (Supelco, Bellefonte, PA, USA) and 10 µl of pyridine (Merck, Darmstadt, Germany) were added and left overnight to derivatize the polar compounds to their trimethylsilyl esters and ethers in order to analyse them by GC-MS. The remaining extract was used for the analysis of PAHs, n-alkanes and hopanes, and was clean-up by adsorption column chromatography, packed with 1 g of aluminium oxide (Merck, Germany). The analytes were eluded with 10 ml of hexane: dichloromethane (1:2 (v/v), Merck, Germany), which was collected and concentrated to 1 ml by rotovap and to 25 µl under a gentle nitrogen stream for quantification by GC-MS (Thermo Trace GC Ultra – DSQ II). The MS detector was operated in full scan (m/z from 50 to 650) and electron impact (70 eV) ionization mode for the polar compounds. The sample extracts for the analysis of non-polar species was performed in selected ion monitoring (SIM) mode

for the corresponding ions of the compounds. Organic species were identified by their GC retention time and characteristic ions in the MS (see section S1 of the supplement).

2.3.2 OC and EC

Organic and elemental carbon (OC and EC) were analysed by thermal-optical transmittance (TOT, Sunset Laboratory Inc. ™) by using the EUSAAR2 protocol (Cavalli et al., 2010). The method provided four OC fractions (OC1, OC2, OC3 and OC4), from which the more volatile were discarded based on the results of the field blank filters analysis. Organic Matter (OM) was determined by using the ratio OM/OC = 1.8 for remote places (Pitchford et al. 2007; Dzepina et al. 2015).

2.3.3 Inorganics

The methodology used for the inorganic speciation is described in detail in Rodríguez et al. (2015). Briefly, soluble species were determined by ion chromatography ($SO_4^{=}$, NO_3^{-}, Cl^{-}) and selective electrode (NH_4^{+}) after water leaching a fraction of filter. Elemental composition was determined by Inductively Coupled Plasma Atomic Emission Spectrometry (ICP-AES, IRIS Advantage TJA Solutions, THERMO™) and Inductively Coupled Plasma Mass Spectrometry (ICP-MS, X Series II, THERMO™) after acid digestion of the sample. Mineral dust was calculated as the sum of Al_2O_3 + SiO_2 + Fe + $CaCO_3$+ K + Na + Mg + P + Ti + Sr (see details in Rodríguez et al., 2011, 2015) and normalized so Al accounts for 8% of the dust mass (see details in Pérez García-Pando et al., 2016). $SO_4^{=}$ was split in non-sea salt sulphate (nss-$SO_4^{=}$) and sea salt sulphate (nss-$SO_4^{=}$ = $SO_4^{=}$ - ss-$SO_4^{=}$) through the relation between marine Na and $SO_4^{=}$. Blank field filters were subject to gravimetric and chemical analysis and mean values subtracted to the PM_x samples.

2.4 Meteorology

The air mass origin and transport was tracked by means of backward trajectory analysis. Calculations were performed with the HYbrid Single-Particle Lagrangian Integrated Trajectory Model (HYSPLIT, http://ready.arl.noaa.gov/HYSPLIT.php; Draxler and Rolph, 2003; Draxler and Hess, 1998; Stein et al., 2015) developed by the National Oceanic and Atmospheric Administration (NOAA). HYSPLIT was run with the National Centre for Environmental Prediction's (NCEP) Global Data Assimilation System (GDAS, 1 degree) data set. Ten days back-trajectories arriving at 2400 m a.s.l were computed daily (00 UTC) for August 2013.

2.5 Data treatment

In order to observe the similarities and differences among the chemical composition of the samples, the experimental organic compound data were merged for evaluation with Multivariate Curve Resolution Alternating Least Squares (MCR-ALS). The joint dataset was imported into MATLAB 7.4 (The Mathworks, Natick, USA) for subsequent calculations using MATLAB

PLS 5.8 Toolbox (Eigenvector Research Inc, Masson WA, USA) (Jaumot et al. 2005). The MCR-ALS method decomposes the data matrix using an Alternating Least Squares algorithm under a set of constraints such as non-negativity, unimodality, closure, trilinearity or selectivity (Tauler et al., 1995a, b). The MCR-ALS method had been applied successfully in a previous study on organic aerosol in urban and rural areas (Alier et al. 2013; Van Drooge and Grimalt 2015). The explained variance by the different components is similar to a PCA, but not orthogonal. Since the natural sources in the environment are rarely orthogonal, the MCR-ALS method provides more realistic descriptions of the components than the orthogonal database decomposition methods. Multilinear regression tools were applied to quantify the contribution of the identified sources to the total OM.

3 Results and Discussion

We collected aerosol samples in four different airflows: 2 FT airflows and other 2 airstreams potentially mixed with BL air. Samples collected at night (PM_T) are representative of the two FT airflows that prevail in this region: the WES and the SAL. As already described, the WES flow from North America across the North Atlantic at mid-latitudes, with their southern edge shifting to the subtropics in winter, and flow over Canada (Merry and Moody, 1996) reaching Izaña after circulation around the Azores high in summer (see backtrajectories of the samples collected from 26Aug to 30Aug – with "ddmmm" referred to ending sampling day – in Fig.1A). The SAL expands from North Africa to the Americas at subtropical latitudes in summertime (see backtrajectories associated during the study period in Fig. 1B), season in which the Izaña Observatory is mostly within this dusty airstream and the presence of the WES is associated with southern shifts of the SAL.

Samples collected during daylight ($PM_{2.5}$) are representative of the FT potentially mixed with BL air, more specifically the BL-SAL mixing and BL-WES mixing. The presence of BL air is associated with the development of buoyant upslope winds caused by the heating of terrain, which typically results in increases of primary gaseous pollutants and new particle formation at Izaña (García et al, 2014; Rodríguez et al., 2009).

Thus, in this study we differentiate between 4 scenarios: PM_T (FT, nightime) within (i) the SAL (FT-SAL) and (ii) the WES (FT-WES), and $PM_{2.5}$ (BL, daytime) within (iii) the SAL (BL-SAL) and (iv) the WES (BL-WES).

3.1 Major Components

Table 1 shows the composition of the aerosol samples collected at Izaña. Concentrations of aerosol major components are the same order to those found in previous studies (Maring et al., 2000; Rodríguez et al., 2011). All species present much higher concentrations within the SAL than within the WES. Some species show slightly higher concentrations during the day linked to the upslope winds and boundary layer air.

3.2 Organic molecular tracers

In the next sections, organic speciation results are described. Table 2 shows the average concentrations of the 40 organic compounds analysed in this study under the different scenarios (SAL and WES) for PM_T and $PM_{2.5}$. In order to improve the insight on the origin and sources of some FT organic aerosol, correlations among the organic groups and the major species are evaluated (Table 3).

3.2.1 Levoglucosan

Levoglucosan (1,6-anhydro-β-D-glucopyranose) is emitted during biomass burning as a consequence of the thermal alteration of cellulose and hemi-cellulose present in vegetation (Simoneit, 2002). It is considered a particle-phase marker for the identification of wood combustion because of its source specific emission, but its atmospheric stability is still a matter of discussion. Experiments carried out by Hennigan et al. (2010) and Hoffmann et al. (2010) showed that levoglucosan reacts with gas-phase hydroxyl radicals (OH), especially under high relative humidity conditions. However, studies performed by Fraser and Lakshmanan (2000) demonstrated no degradation of levoglucosan under acidic conditions over a period of 10 days.

Levoglucosan daily values measured at Izaña within the FT and the BL were < 1.5 $ng \cdot m^{-3}$ for all samples, except on 28Aug when ~9 $ng \cdot m^{-3}$ was measured. Hysplit back-trajectories and the Atmospheric Infrared Sounder (AIRS) satellite images (NASA) indicate the North America origin of the air masses, where several wildfires – as the Rim Fire – were affecting western USA 10 days before the arriving of the air mass towards Izaña (detailed information not provided for sake of brevity). We detected a long-range transport biomass burning plume within the FT from the fires originated in North America. Other studies performed at Pico Mountain Observatory (Azores, 2225 m a.s.l.) have also detected the impact of other biomass burning plumes by means of the levoglucosan detection (Dzepina et al, 2015). These results give support to the atmospheric stability of levoglucosan, for the specific conditions of the atmospheric long-range transport. Due to the particular composition of this biomass burning event (BBE), we will discuss this sample separately (Table 2) and the sample will not be included when describing the general composition of the samples collected at night under conditions of the westerlies (FT-WES; Table 2). Levoglucosan concentration, measured at Izaña during the BBE (9.3 $ng \cdot m^{-3}$), is similar to the average levels detected in the marine BL on the Azores in the North Atlantic (5.2 $ng \cdot m^{-3}$) or at free tropospheric site in the European continent (7.8 $ng \cdot m^{-3}$), but much lower than those found in sites under influence of local BB or continental sites in winter (653–1290 $ng \cdot m^{-3}$) (Puxbaum et al. 2007).

3.2.2 Dicarboxylic acids

Dicarboxylic acids can be emitted in small quantities from several natural and anthropogenic primary sources such as vegetation, meet cooking and motor exhaust emissions (Kawamura and Kaplan, 1987, Narukawa et al., 1999), although atmospheric photochemical transformation of volatile and semi-volatile organic compounds is considered to be an important

source for the presence of these aged compounds in the atmosphere (Alier et al. 2013, Jang and McDow, 1997; Kleindienst et al. 2012; Paulot et al. 2011). This oxidative degradation of VOCs by tropospheric oxidants may be responsible for the similar mean ∑dicarboxylic acids concentrations within the FT (SAL: 14.4 ng·m^{-3}; WES: 16.7 ng·m^{-3}) and the BL (SAL: 11.1 ng·m^{-3}; WES: 12.9 ng·m^{-3}) at Izaña.

Succinic (suc) and phthalic (pth) acids were the most abundant dicarboxylic acids (Table 2) with FT and BL average values (suc: 6.5–3.7 and pth: 3.2–2.8 ng·m^{-3} for the FT-BL) much lower than this found for $PM_{2.5}$ in the FT Mount Tai (suc: 30 ng·m^{-3}; Wang et al., 2009), similar to those observed in PM_T in the Himalayas (4276 m a.s.l.) (suc: 13.7 and pth: 9.5 ng·m^{-3}; Cong et al., 2015), but higher than those detected for PM_T in the North Pacific remote marine (suc: 2.8 and pth: 0.66 ng·m^{-3}; Kawamura and Sakaguchi., 1999). Malic acid within the BL (the third most abundant poly-acid at Izaña; Table 2) might have a photochemical origin via OH oxidation of the surrounding biogenic compounds transported by the day-time upslope winds. The Izaña Observatory is surrounded downhill by a forest ring – an important source of biogenic volatile organic compounds (BVOCs) – which contributes significantly to the measured concentrations at Izaña. Oxidation of these biogenic precursors may also provide important amounts of C_7–C_9 dicarboxylic acids.

High concentrations of dicarboxylic acids have been reported in plumes from BB (Narukawa et al., 1999; Gao et al., 2003), which is in agreement with the observed values for the long-range transport BBE (82 ng·m^{-3}). Concentrations of succinic, glutaric and malic acids were high (~33 ng·m^{-3}, ~7 ng·m^{-3} and ~32 ng·m^{-3}, respectively; Table 2), compared to the rest of the period, surely as a consequence of the lofted concentration emitted in the open fire and long-range transport photochemical aging processes.

3.2.3 Saccharides

Primary saccharides and polyols are tracer compounds of surface soils (Medeiros and Simoneit 2007; Simoneit et al. 2004a), related to plant tissue and microorganisms. Glucose (α, β), fructose and sucrose are important constituents of OM in soils (Simoneit et al. 2004a), whereas mannitol is related to airborne fungal spores (Bauer et al. 2008). They are completely water-soluble, contributing to water soluble organic carbon (WSOC) in aerosols (Simoneit et al. 2004a). Wind erosion and up whirling of soil dust emit these compounds to the atmosphere (Simoneit et al. 2004a).

The average concentration of the saccharides exhibits a marked difference within the FT-PM_T (23.5 ng·m^{-3}) and the BL-$PM_{2.5}$ (3.5 ng·m^{-3}). Previous studies have shown that some organic compounds are strongly particle size dependent Mochida et al., 2003; Van Drooge and Grimalt, 2015), with special emphasis in sugars and sugar alcohols which are present mostly in very large particles (Graham et al., 2003; Yttri et al., 2007). This size-segregation is clearly seen for the $PM_{2.5}$ samples collected within the BL, that cut off an important fraction of the coarse organic soil dust aerosol, showing similar concentrations under SAL and WES influence (BL-SAL = 3.3 ng·m^{-3}; BL-WES = 4.0 ng·m^{-3}). A different scenario takes

place with the PM_T samples, for which concentrations rise one order of magnitude from SAL influence to clean conditions (FT-SAL = 27 ng·m^{-3}; FT-WES = 2.5 ng·m^{-3}) linked to Saharan dust contribution. The average saccharides levels in the FT-SAL are higher than these observed in a natural forest area in tropical India (12.78 ng·m^{-3}; Fu et al., 2010) and a rural background in Norway (10.4 ng·m^{-3}; Yttri et al., 2007), but very similar to the average concentrations measured in the FT over central china (28.1 ng·m^{-3}; Fu et al., 2014).

Glucose (α+β) was the predominant saccharide within the SAL, with mean FT concentration of ~10 ng·m^{-3} (Table 2); both isomers showed a good correlation (R^2= 0.998) consistent with their relation in the soil (Simoneit et al. 2004a). Under the WES airflows, glucose (α+β), sucrose and mannitol were slightly higher during the day (BL; Table 2), suggesting that there might be some soil contribution of transported terrestrial OM by land breeze. This load is more evident in the sucrose (FT-WES = 0.3 ng·m^{-3}; BL-WES = 1.3 ng·m^{-3}; Table 2), which is a predominant sugar in the phloem of plants playing a key role in developing flowers (Bieleski et al., 1995) and has been suggested as a tracer for airborne pollen grains (Fu et al., 2012).

3.2.4 n-Alkanes

n-Alkanes, or aliphatic hydrocarbons, are a result of biogenic and anthropogenic emissions such as plant waxes and fossil fuel combustion products (Mazurek et al. 1989; Simoneit et al. 1991; Shauer et al. 2002). In the present study n-alkanes from nC_{24} to nC_{34} were quantified, with total n-alkanes mean concentrations (~8 ng·m^{-3} in the FT and in the BL) much lower than this measured in the tropical Indian summer (126 ng·m^{-3}; Fu et al., 2010), but similar to this found in rural Spain during the warm period (12 ng·m^{-3}; Van Drooge and Grimalt, 2015).

Information about the possible source can be provided by the carbon number maximum (C_{max}). In general, nC_{27}, nC_{29} and nC_{31} are related to waxes from terrestrial higher plants, whereas low-molecular-weight alkanes (C_{22}–C_{25}) are more associated to combustion sources (Mazurek et al. 1989). At Izaña, the most abundant n-alkanes within the FT-SAL were nC_{27}, nC_{29} and nC_{31} (~1.0 ng·m^{-3}, ~1.4 ng·m^{3} and ~1.8 ng·m^{-3} respectively; Table 2) reflecting a vegetative source as previously described for Saharan dust samples measured in the North Atlantic (Simoneit et al., 1977), whereas within the BL nC_{24}–nC_{25} presented the higher concentrations (Table 2) linked to anthropogenic emissions carried by the upslope winds. Another indicator that can be used to show the type of source is the carbon preference index (CPI = ∑odd n-alkanes / ∑even n-alkanes) with CPI > 1 related to biogenic origin and CPI ≈1 to combustion processes (Mazurek et al. 1989; Simoneit, 2002). In this study, CPI values ranged from 0.9 to 6.3 with average values for the FT-SAL (~2) higher than for the BL (~1.7) and the FT-WES (~1.2), reflecting the larger influence of vegetation within the FT-SAL and the predominance of combustion contribution within the BL and FT-WES samples. Although the vegetative source dominates in the FT, there is a significant correlation between n-alkanes and NO_3^- (r = 0.8, p<0.01; Table 3), mostly due to its anthropogenic fraction (C_{24}–C_{25}).

3.2.5 Hopanes

Hopanes (17α(H),21β(H)-29-norhopane and 17α(H),21β(H)-hopane) are linked to mineral oil and related to unburned lubricating residues from primary vehicles emissions (Rogge et al., 1993; Schauer et al., 1996, 2002). ∑Hopanes mean concentrations were 0.13 and 0.08 ng·m^{-3} within the FT and BL respectively, values much higher than the 7·10^{-4} ng·m^{-3} measured by von Schneidemesser et al. (2009) in remote Greenland (3200 m a.s.l.) where anthropogenic emissions in the surrounding region are minimal. Under the WES airflows, hopanes concentrations were slightly higher during the day, suggesting influence of pollution transported within the BL, related to motorized vehicle emissions. The quantified hopane and norhopane showed very good linear correlations (R^2= 0.95), pointing to the same emission sources.

A strong correlation is observed in the FT between hopanes and NO_3^- (r = 0.8, p<0.01; Table 3) suggesting that most of NO_3^- in the FT has its origin in on-road vehicle emissions instead of the industry. Anthropogenic sources of NO_x (the major NO_3^- precursor) include fossil fuel emitted from agriculture, power plants, industry and transport. The latter one covers almost a 50% of the nitrogen oxides emissions (http://www. eea.europa.eu/data-and-maps/indicators/eea-32-nitrogen-oxides-nox-emissions-1/assessment.2010-08-19. 0140149032-3), with on-road transport in 2010 being the highest (25.2 Tg·year^{-1}) compared to non-road (10.1 Tg·year^{-1}), shipping (16.2 Tg·year^{-1}), aviation (3.0 Tg·year^{-1}) or rail (1.6 Tg·year^{-1}) (Yan et al., 2014).

3.2.6 Polycyclic aromatic hydrocarbons

Polycyclic aromatic hydrocarbons (PAH) are organic pollutants generated during incomplete combustion of organic material natural (e.g. forest fires, volcanic activity) and anthropogenic (e.g. fossil fuels combustion, coke production) sources (Howsam and Jones 1998; Iinuma et al., 2007; Rogge et al., 1993; Schauer et al., 1996, 2002). PAHs are composed of two or more fused aromatic rings and some of them have carcinogenicity, genotoxicity, and potential endocrine disruptiveness, affecting human health. At Izaña mean values of the total PAHs exhibited higher values in the BL (24 pg·m^{-3}) than in the FT (16.3 pg·m^{-3}), reflecting the contribution of the upslope winds as described for other organic compounds.

Similar PAHs concentrations were previously found by van Drooge et al. (2010) who measured an average PAHs concentration of 33.1 pg·m^{-3} at Izaña. In general, all individual PAHs decreased its concentration except benz(a)anthracene that increased by a factor of 1.5 and 1.35 with respect to the mean concentrations of the FT and BL correspondingly. Much higher concentrations have been reported in other remote FT locations as Mt. Tai (1534 m a.s.l.) where ~9 ng·m^{-3} were measured (Fu et al., 2008). In the FT there is a strong correlation between PAHs and EC (r = 0.7, p<0.01; Table 3), which points to the incomplete combustion of fossil fuels (Frenklach., 2000).

During the detected North America wildfire event (28Aug), PAHs concentration was 9.4 pg·m^{-3}, which is much lower than levels measured in Thailand for PM_T samples during BBEs in the dry season (1150 to 4140 pg·m^{-3}; Chuesaard et al., 2014). The concentrations of PAHs measured in the sample corresponding to the fire event were not higher than those observed in

the other samples, which may be due to photochemical transformations of PAH in the atmosphere during long-range transport.

3.2.7 Tracers of α-pinene oxidation (SOA PIN)

Vegetation emit large quantities of biogenic volatile organic compounds (BVOCs) into the atmosphere compared to anthropogenic VOCs (Guenter et al., 2006, 2012; Lamarque et al., 2010), particularly monoterpenes and isoprene. The most abundant volatile monoterpene, emitted mainly by coniferous trees (i.e. *Pinus canariensis*) is α-pinene (Andreani-Aksoyoglu and Keller, 1995; Rinne et al., 2009; Smolander et al., 2014) and the tracers related to its photochemical oxidation (SOA PIN) are *cis*-pinonic acid, 3-hydroxyglutaric acid (3-HGA) and 3-methyl-1,2,3-butanetricarboxylic acid (MBTCA) (Claeys et al., 2007; Szmigielski et al., 2007).

SOA PIN organic tracers were not detected in all samples, with values in the FT influenced by a couple of extreme points that increased their average concentration. SOA PIN exhibited the lowest concentration in the FT-WES (1.2 $ng \cdot m^{-3}$) with a predominance of *cis*-pinonic acid (Table 2). Aircraft measurements in the FT over central China (Fu et al., 2014) recorded higher concentrations of 3-HGA (8.5 $ng \cdot m^{-3}$) and MBTCA (1.9 $ng \cdot m^{-3}$) than measure in the present study (Table 2). Further generation oxidation products (3-HGA and MBTCA) were higher in the BL (0.51 and 0.24 $ng \cdot m^{-3}$ correspondingly; Table 2), with a significant correlation (R^2 = 0.81) that points to a same precursor. Monoterpenes reacts relatively fast, with atmospheric lifetimes ranging from minutes to hours (Saxton et al., 2007), resulting in *α*-pinene emitted in the ring forest that reacts along its upward transport to the Observatory. Daytime emissions of gaseous α-pinene at Izaña were measured by Fisher at al. (1998) with concentration in the range of 0.011–0.102 ppbv (mean: 0.028 ppbv), supporting the evidence of its origin close to the Observatory during the day.

3.2.8 Tracers of isoprene oxidation (SOA ISO)

It is estimated that about a half of the total global BVOCs emission is due to isoprene (535 $Tg \cdot y^{-1}$; Guenter et al., 2012), making it the largest BVOC emitted from land vegetation (Guenter et al., 2006). Isoprene emission is limited to a number of species in the plant kingdom, contrary to many other BVOCs that are emitted from most plants (Guenter et al., 2012). Secondary products of isoprene oxidation (SOA ISO) evaluated in the present study are 2-methylglyceric acid (2-MGA), 2-methylthreitol (2-MT1) and 2-methylerythritol (2-MT2) (Claeys et al., 2004; Hallquist et al., 2009).

Analogous FT concentrations of 2-methylthreitol and 2-methylerythritol were measured in the present study under the SAL (7.3 and 16.8 $ng \cdot m^{-3}$; Table 2) and over the central China FT (8 and 17 $ng \cdot m^{-3}$; Fu et al., 2014), one of the most important source regions of isoprene emission in the world during summertime (Guenther et al., 1995). Similar SOA ISO concentrations were found in the BL within the SAL and the WES (~17 and ~16 $ng \cdot m^{-3}$ respectively) revealing the emission and following ascending transport of biogenic or anthropogenic compounds, as found in previous studies performed at Izaña,

which observed emissions of isoprene during daytime associated to anthropogenic compounds (Salisbury et al., 2006). A significant correlation among 2-MT1 and 2-MT2 was found for individual values (R^2 = 0.94) as previously observed in other studies (Ion et al., 2005; El Haddad et al., 2011), but with a mass concentration ratio 2-MT1 vs. 2-MT2 (slope from linear regression=2.3) slightly lower than this found by El Haddad et al. (2011). This correlation between the two diastereoisomers indicates a same origin thought the same photo-oxidation process.

The highest concentration of SOA ISO was measured under the FT-SAL (~28 ng·m^{-3}), associated to Saharan dust, as was observed for SOA PIN (~33 ng·m^{-3}). However, global estimations of isoprene and α-pinene emissions and sources show they are diverse and not equally distributed in the globe (Luo et al., 2010; Guenther et al., 2012; Sindelarova et al., 2014). Correlation between total concentration of SOA ISO and total concentration of SOA PIN (Fig. 2) exhibits two distinct trends in the FT that might be associated to different global sources of the precursor volatile compounds, although the trajectories of the sampled air mass does not distinguish clearly between different origins. Some species with a high isoprene emission potential have been identified in central and western Africa, but quantification of isoprene emissions are largely unverified for West Africa (Saxton et al., 2007). Several evaluations of isoprene and α-pinene global emissions (Luo et al., 2010; Guenther et al., 2012; Sindelarova et al., 2014) confine the North Africa sources to a small belt over the northern part of Morocco, Algeria and Tunez, whereas Europe is pointed as a potential source. Some episodes, for which SOA PIN and SOA ISO were measured, do not have a trajectory over this African belt – based on the Hysplit model – , suggesting that air masses from Europe can also incorporate gaseous precursors and oxidized species previous to its pass over Africa and Izaña in the Atlantic Ocean.

Rodríguez et al. (2011) previously reported high concentrations of $SO_4^{=}$, NO_3^- and NH_4^+ for air masses arriving to Izaña from the Atlantic coast of Morocco, Eastern Algeria, Northern Algeria and Tunisia. Industrial states with sources of gaseous precursors (SO_x, NO_x and NH_3) of these aerosol compounds were identified. Although African emissions seem to be responsible of the pollutants arriving to the North Atlantic FT, Europe could also contributes with an amount of pollutants that should not be neglected as evidenced by the concentration of SOA PIN and SOA ISO arriving to Izaña. These species could play a key role in secondary organic aerosol formation, as some studies point to the influence of anthropogenic emission on secondary organic aerosol formation (El Haddad et al., 2011; Hoyle et al., 2011). SOA ISO seems to depend strongly on the conditions (aerosol acidity, NO_x concentrations and pre-existing aerosol) used to oxidize isoprene (Surratt et al., 2006, 2007; Marais et al., 2016). NO_x concentration determine the pathway (low-NOx and high-NOx) followed by the isoprene oxidation, leading to different secondary organic species (Paulot et al., 2009a, b); the low-NOx pathway is ~ 5 times more efficient than the high-NOx pathway (Marais et al., 2016). Experiments carried out by Kroll et al. (2006) evidence how the isoprene SOA yield varies depending on NOx concentration, increasing from no injected NOx, to a plateau between 100 and 300 ppb NOx, and decreasing at higher NOx concentrations.

We found the relation among SOA ISO and NO_3^- within the FT-SAL (Fig.3) present three tendencies which might be associated to the ratio isoprene:NO_x in the source. The different correlation are supported by the fact that the SOA ISO markers (2-MTs and 2-MGA) do not exhibit the same temporal trend (FT-SAL 2-MTs us 2-MGA-r^2: 0.1), which has been suggested to be linked to the NOx concentration influence on this SOA ISO markers formation pathways (El Haddad et al., 2011). The high-NOx pathway leads to the reaction of isoprene peroxy radicals (iRO_2) with NO resulting in carbonyls and hydroxynitrates production (Surratt et al., 2006), whereas the low-NOx pathway leads to the reaction of iRO_2 with hydroperoxy radicals (HO_2) resulting in hydroxyhydroperoxides (iROOH), and carbonyls production to a lesser extent (Carlton et al., 2009; Paulot et al., 2009). This has implication on the abundance of the secondary organic markers from isoprene photo-oxidation (2-MT and 2-MGA): high-NOx pathway results in the major product 2-MGA and low-NOx is associated to the major products 2-MTs (El Haddad., 2011).

Significant correlations in the FT between biogenic secondary organic compounds and NO_3^- (r SOA PIN–NO_3^- = 0.6, $p<0.01$; Table 3) and nss-$SO_4^=$ (r SOA ISO–nss-$SO_4^=$ = 0.6, $p<0.01$; Table 3), point to its formation from the oxidation of their gaseous precursors NO_x and SO_2 respectively. Dust transformation in the FT is also evidenced by its highly significant correlation with SOA PIN (r = 0.7, $p<0.01$; Table 3) as well as both saccharides (r = 0.6, $p<0.01$) and hopanes (r = 0.9, $p<0.01$) showing that natural and anthropogenic substances might be mixed after aging processes.

3.2.9 Determined fraction of OM

Bulk organic carbon (OC) determined for every single day (thermo-optical transmittance method) at Izaña during this study was within the range 0.01–2.20 $\mu g \cdot m^{-3}$, which is of the order to that found in other FT studies (e.g. 1.4 $\mu g \cdot m^{-3}$ at Qomolangma, Mt. Everest, 4276 m a.s.l. by Cong et al., 2015 and 4 $\mu g \cdot m^{-3}$ at NW Pacific, 2–6.5 km column by Heald et al., 2005). FT-PM_T OC under SAL conditions (0.77 $\mu g \cdot m^{-3}$) was higher than under WES (0.52 $\mu g \cdot m^{-3}$, including the BBE) events. Figure 4 shows the mass closure (sum of the organic species determined by speciation) of bulk organic matter OM (determined as OC·1.8); this mass closure accounts for 2 to 100 % of the OM for every single day, depending on the sample and the airflows.

Concentrations of OM were much higher in the FT-SAL (1.39 $\mu g \cdot m^{-3}$) than under FT-WES (0.04 $\mu g \cdot m^{-3}$ without the BBE; 0.94 $\mu g \cdot m^{-3}$ including the BBE) conditions. The selected tracers (levoglucosan, SOA ISO, SOA PIN, n-Alkanes, saccharides, dicarboxylic acids, hopanes and PAHs) represent as average:

(i) a 15% of the OM (Fig. 4), under FT-SAL conditions (when mean OM was 1.39 $\mu g \cdot m^{-3}$). This determined fraction is mainly composed by SOA ISO (30%), saccharides (27%) and dicarboxylic acids (18%).

(ii) a 84% of the OM (Fig. 4), in the FT-WES airflows without the BBE (when mean OM was 0.04 $\mu g \cdot m^{-3}$). This determined fraction is constituted by dicarboxylic acids (44%; mainly succinic and phthalic, indicating aged

aerosols after the long-range atmospheric transport), and SOA ISO (34%) with a minor presence of saccharides (8%). Biogenic SOA represent an important fraction of the OM at Izaña (~40%), as seen in other remote high altitude regions (Xu et al. 2015).

(iii) a 3% of the OM (Fig. 4) in the FT-WES during the BBE (when mean OM was 3.64 $\mu g \cdot m^{-3}$). The determined fraction of OM for 28Aug (3%) contained a 68% of dicarboxylic acids (mostly succinic and malic acids) and an 8% of the BB tracer levoglucosan. This sample has the OM profile with the highest contribution of aged SOA (di-acids), formed during the long-range atmospheric transport, and the lowest contributions of SOA PIN (4%) and SOA ISO (12%), which could indicate the further oxidation of these products under the BBE air masses conditions.

(iv) a 64% of the OM in the FT-WES including the BBE (when mean OM was 0.94 $\mu g \cdot m^{-3}$). This determined fraction is constituted mainly by dicarboxylic acids (50%), and SOA ISO (28%).

Differences in the determined fraction of the samples collected under the FT-SAL and FT-WES influence – as observed in Fig. 4 – is a result of the method limitation, as the analysis of the samples by means of gas chromatography–mass spectrometry (GC-MS) covers a very small fraction (often < 5 %; Alier et al., 2013) of the organic matter. The determined OM composition within the BL ($PM_{2.5}$; BL-FT: 9% of the OM and BL-WES: 77% of the OM; Fig. 4) remains almost the same under both airflows, but with higher concentrations of SOA ISO and n-alkanes under the SAL. However, due to the $PM_{2.5}$ cut-off of the collected particles, the influence of the dust-associated organic compound is probably not well represented since these products are situated in the coarse fraction of the PM.

3.3 Sources of OM

We used receptor modelling for apportioning OM between the OA sources traced by the species included in the speciation performed in this study. This analysis is complementary to the mass closure performed above (Fig.4). The data matrix was decomposed in two factors: loadings (i.e. the relative amount of the chemical compounds in the source) and scores (i.e. the relative contribution of the potential sources to the organic aerosol) (Tauler et al., 2009). The loading factors obtained in the MCR-ALS were used to identify OA sources (Fig.5A1–5C1), whereas the score factors were used as independent variables in the Multilinear Regression Analysis (MLRA) to apportion the determined fraction of OM between the identified sources. Three components (sources) were identified (Fig. 5), which accounted by 81% of the total variance. MCR-ALS method was also applied only to PM_T samples to verify the influence of $PM_{2.5}$ in the final results; no significant differences were observed as shown in Fig. S1 of the supplement.

3.3.1 Biomass Burning (BB)

The major component (accounting for 63% of the total variance) is associated with levoglucosan, dicarboxylic acids, phthalic acid, SOA PIN, C_{24}–C_{28} alkanes and hopanes and PAHs to a lesser extent (Fig. 5A). This factor represents biomass burning aerosols (BB). The peak event in the score factor observed the 28Aug (Fig. 5A2) is associated with the episode of levoglucosan linked to the long-range transport of BB from North America. SOA PIN indicates photochemical oxidation of biogenic volatile organic compounds during the wild fire. The presence of short-chain dicarboxylic acids, along with important amounts of malic acid, suggests the effective oxidation of organic species to shorter di-acids chains during long-range atmospheric transport. PAH contribution in this component is low, despite potential emissions of PAHs during biomass burning. The low PAH contributions could be the result of photochemical degradation during long-range transport, which on their term could be related to the presence of higher contributions of phthalic acid in this component. BB in the FT is significantly associated to the OM (r-FT = 0.40, $p < 0.05$; Table S1) and EC (r-FT = 0.65, $p < 0.01$; Table S1) concentrations.

3.3.2 Combustion POA

The second component (accounting for 21% of the total variance) is associated with long-chain dicarboxylic acids, SOA ISO, $C_{24} - C_{29}$ n-alkanes and PAHs (Fig. 5B). This factor is related to the primary organic aerosols linked to combustion sources. This is the component that best represents the variability of $PM_{2.5}$ samples collected during daylight, when the BL may reach Izaña under the slope wind regime. High loadings of suberic (C_8) and azelaic acids (C_9) indicate the presence of oxidized compounds in the early stage of photochemical transformation processes, such as the ozonolysis of oleic acid (Moise and Rudich, 2002). Organic species supporting the anthropogenic contribution are lower-molecular-weight n-alkanes ($C_{24} - C_{25}$) and PAHs (from incomplete combustion processes). FT aerosol is also described by this component with the exception of low-molecular-weight alkanes (C_{24}–C_{25}) which is the main feature of the BL samples. The component is significantly representative of the measured EC for all samples, and highly representative for the BL, as shown by its Pearson correlation coefficient (r-All = 0.36 and r-BL = 0.71, $p < 0.05$; Table S1).

3.3.3 Organic dust

The third component, accounting for 16% of the total variance, is composed by short-chain dicarboxylic acids, SOA ISO, saccharides, C_{26}–C_{34} alkanes, hopanes, and PAHs to a lesser extent (Fig. 5C). This component, identified as organic dust, is associated with soil re-suspension as evidenced by the saccharides and mannitol high loadings. The predominant presence of the soil OM related compounds, those form fungi and terrestrial higher plants (C_{27}, C_{29} and C_{31}), suggest fresh and primary OA. Notwithstanding, glutaric, adipic and pimelic acids indicate oxidation products, suggesting the aging of the samples. As a consequence of this aging, natural and anthropogenic markers are mixed in this component. The biogenic influence is indicated by the presence of soil related markers and oxidation products from isoprene (2MGA, 2MT-1 and 2MT-2), whereas the anthropogenic influence is well defined by the presence of hopanes (primary vehicle emissions) and high

molecular weight PAH (products of incomplete combustion). The scores of this component display the highest correlation with dust (r-All = 0.84, $p < 0.01$; Table S1) and OM (r-All = 0.64, $p < 0.01$; Table S1) concentrations for all samples. Although this component is not relevant for the BL-$PM_{2.5}$ samples – because of part of the compounds are present in the larger particle size fractions – the correlation with dust (r-BL = 0.73, $p < 0.01$; Table S1) and OM (r-BL = 0.75, $p < 0.01$; Table S1) are highly significant due to the mixing of dust with the anthropogenic compounds.

3.3.4 Source apportionment of OM in the SAL and the westerlies

The source apportionment of OM was performed by the multilinear regression technique described above. The difference between the bulk OM (determined by thermo-optical method) and the sum of the organic species (determined with the speciation) was labelled as undetermined fraction. Figure 6 shows the time series of the daily contribution of each source to the determined OM and Fig. 7 shows the average source contribution to total OM in the aerosol samples collected in the different airstreams. The correlation between the sum of the three components scores and the OM within the FT (OM r-FT = 0.63; Table S1) indicates that the identified sources might describe, not only the determined fraction of the OM but also the total OM. This significant correlation is not seen for the BL (OM r-BL = 0.33; Table S1), where there could be additional sources.

In the FT-SAL airflow, most of OM was undermined (~85, Fig.7). The three identified sources, i.e. the organic dust, combustion POA and biomass burning, accounts for 8%, 6% and 1% of the bulk OM, respectively (62%, 34% and 4% of the determined OM, respectively). The presence of biogenic SOA products mixed with combustion POA was also found in previous studies which suggested that biogenic SOA formation may be more efficient in polluted atmospheres (Gouw and Jiménez., 2009 and references therein).

In the FT-WES, the undermined fraction accounts for ~36% of the OM (Fig.7). The contribution of the three identified sources, i.e. the organic dust, combustion POA and biomass burning, is 22%, 19% and 23% to the bulk OM, respectively (28%, 23% and 49% to the determined OM, respectively). Yttri et al. (2007) proposed biomass burning as a source of saccharides in the OA and Fraser and Lakshmanan (2000) found that some saccharides resist degradation in the atmosphere over a period of 10 days, being able to be transported over long distances; this may be the source of the organic fraction of dust we detected in the FT-WES.

For the BL samples, the dust related component is not well represented (Fig. 6), because the coarse fraction was not sampled here. On the other hand, combustion POA explains a 6 and 41 % (Table S2) of the bulk OM for the SAL and WES, respectively. Background regional fires also affect the BL as described by the BB component, which represent a 2 and 36 % (Table S2) of the bulk OM for the SAL and WES, respectively.

4 Conclusions

The present study is focused on the organic aerosol composition within the two main airflows of the subtropical North Atlantic free troposphere: (i) the Saharan Air Layer – the warm, dry and dusty airstream that expands from North Africa to the Americas at subtropical and tropical latitudes – and (ii) the westerlies – which flows from North America through the North Atlantic at mid and subtropical latitudes –. Atmospheric particulate matter was analysed on secondary inorganic species, elemental composition, elemental and organic carbon and 40 organic tracer species (levoglucosan, dicarboxylic acids, saccharides, n-alkanes, hopanes, polycyclic aromatic hydrocarbons and those formed after oxidation of α-pinene and isoprene) in order to distinguish possible sources for the organic aerosol. The organic particulate aerosol speciation and its subsequent source apportionment was performed for 42 filter samples collected in summer at the Izaña Observatory (~2400 m a.s.l.) in Tenerife, Spain.

The levels of all inorganic and almost all organic tracers were generally higher under the Saharan Air Layer influence in comparison to the pristine conditions of the Westerlies and the differences in the composition of the determined organic matter under these two air masses were important.

In the Saharan Air Layer, the aerosol composition was dominated by dust (93%), secondary inorganic pollutants (<5%) and organic matter (~1.5%). The organic compounds (determined by gas-chromatography coupled to mass-spectrometry) accounted for a 15% of the bulk organic matter and were related to soils (saccharides), biogenic secondary organic aerosols linked to isoprene oxidation (SOA ISO) and natural and anthropogenic primary sources such as vegetation and motor exhaust emissions (dicarboxylic acids).

In the Westerlies, the organic matter represented a higher fraction of the total aerosol bulk (~28%) and the determined organic compounds accounted for an 64% of the organic matter with dicarboxylic acids and SOA ISO being the most abundant. In this airstream, a long-range atmospheric transport of a biomass burning plume from North America was detected (with organic matter representing a 53% of the total aerosol bulk), supporting the atmospheric stability of levoglucosan over transport and time under certain conditions.

Three sources of organic aerosol, which contribute to the organic matter composition in this part of the North Atlantic, could be resolved in multivariate analysis: one biomass burning-related, one primary combustion-related and one organic dust-related. In the Saharan Air Layer, the organic matter comes from organic dust (8% of the bulk OM; 63% of the determined OM) and combustion (6% of the bulk OM; 34% of the determined OM) sources, whereas under the westerlies comes from organic dust (22% of the bulk OM; 28% of the determined OM), biomass burning (23% of the bulk OM; 49% of the determined OM) and combustion (19% of the bulk OM; 23% of the determined OM) sources, showing that the free troposphere is highly influenced by combustion and biomass burning compounds.

A comprehensive knowledge of the organic aerosol chemistry is of high importance for assessing anthropogenic influences and evaluating the effect of radiative forcing. The work presented here offers new insights into the organic composition of the North Atlantic free troposphere as well as the trans-boundary origin of some compounds. Further studies are needed to understand the main mechanisms by which the aerosol is lofted into the free troposphere and transported over long distances.

Acknowledgements: This study was performed within the context of the projects AEROATLAN (CGL2015-66299-P; MINECO/FEDER) and TEAPARTICLE (CGL2011-29621), supported by the Ministry of Economy and Competitiveness of Spain and the European Regional Development Fund (ERDF). The authors acknowledge the NOAA Air Resources Laboratory (ARL) for the provision of the HYSPLIT back-trajectories used in this publication. The excellent work performed by the staff of the Atmospheric Research Centre (C. Bayo, C. Hernández, F. de Ory, V. Carreño, R. del Campo and SIELTEC Canarias) and of the Institute of Environmental Assessment and Water Research (R. Chaler, D. Fanjul, and B. Hortelano) is appreciated. M. I. García acknowledges the grant of the Canarian Agency for Research, Innovation and Information Society (ACIISI) co-funded by the European Social Funds. Measurements at Izaña observatory are performed within the context Global Atmospheric Watch networks with the financial support of the State Meteorological Agency of Spain (AEMET).

Competing interests: The authors declare that they have no conflict of interest.

Gobierno de Canarias
Agencia Canaria de Investigación, Innovación y Sociedad de la Información

canarias OBJETIVO de PROGRESO
Unión Europea
Fondo Social Europeo

European Regional Development Fund

References

Alier, M., van Drooge, B. L., Dall'Osto, M., Querol, X., Grimalt, J. O. and Tauler, R.: Source apportionment of submicron organic aerosol at an urban background and a road site in Barcelona (Spain) during SAPUSS, Atmos. Chem. Phys., 13 (20), 10353–10371, doi:10.5194/acp-13-10353-2013, 2013.

Andreani-aksoyoglu, S. and Keller, J.: Estimates of monoterpene and isoprene emissions from the forests in Switzerland, J. Atmos. Chem., 20 (1), 71–87, doi:10.1007/BF01099919, 1995.

Bauer, H., Claeys, M., Vermeylen, R., Schueller, E., Weinke, G., Berger, A. and Puxbaum, H.: Arabitol and mannitol as tracers for the quantification of airborne fungal spores, Atmos. Environ., 42 (3), 588–593, doi:10.1016/j.atmosenv.2007.10.013, 2008.

Bieleski, R.: Onset of phloem export from senescent petals of daylily, Plant Physiol., 109, 557–565, 1995.

Birch, M. E. and Cary, R. A.: Elemental carbon-based method for monitoring occupational exposures to particulate diesel exhaust, Aerosol Sci. Technol., 25, 221–241, doi: 10.1080/02786829608965393, 1996.

Boose, Y., Sierau, B., García, M. I., Rodríguez, S., Alastuey, A., Linke, C., Schnaiter, M., Kupiszewski, P., Kanji, Z. A., and Lohmann, U.: Ice nucleating particles in the Saharan Air Layer, Atmos. Chem. Phys., 16, 9067-9087, doi:10.5194/acp-16-9067-2016, 2016.

Brown, S. S., de Gouw, J. A., Warneke, C., Ryerson, T. B., Dubé, W.P., Atlas, E., Weber, R. J., Peltier, R. E., Neuman, J. A., Roberts, J. M., Swanson, A., Flocke, F., McKeen, S. A., Brioude, J., Sommariva, R., Trainer, M., Fehsenfeld, F. C., and Ravishankara, A. R.: Nocturnal isoprene oxidation over the Northeast United States in summer and its impact on reactive nitrogen partitioning and secondary organic aerosol, Atmos. Chem. Phys., 9, 3027–3042, doi:10.5194/acp-9-3027-2009, 2009.

Carlton, A. G., Wiedinmyer, C., and Kroll, J. H.: A review of Secondary Organic Aerosol (SOA) formation from isoprene, Atmos. Chem. Phys., 9, 4987–5005, doi:10.5194/acp-9-4987-2009, 2009.

Cavalli, F., Viana, M., Yttri, K. E., Genberg, J., and Putaud, J.-P.: Toward a standardised thermal-optical protocol for measuring atmospheric organic and elemental carbon: the EUSAAR protocol, Atmos. Meas. Tech., 3, 79-89, doi:10.5194/amt-3-79-2010, 2010.

Chuesaard, T., Chetiyanukornkul, T., Kameda, T., Hayakawa, K. and Toriba, A.: Influence of Biomass Burning on the Levels of Atmospheric Polycyclic Aromatic Hydrocarbons and Their Nitro Derivatives in Chiang Mai, Thailand. Aerosol Air Qual. Res. 14: 1247–1257, 2014.

Claeys, M., Graham, B., Vas, G., Wang, W., Vermeylen, R., Pashynska, V., Cafmeyer, J., Guyon, P., Andreae, M. O., Artaxo, P. and Maenhaut, W.: Formation of secondary organic aerosols through photooxidation of isoprene., Science, 303(5661), 1173–1176, doi:10.1126/science.1092805, 2004.

Claeys, M., Szmigielski, R., Kourtchev, I., Van der Veken, Pi., Vermeylen, R., Maenhaut, W., Jaoui, M., Kleindienst, T., Lewandowski, M., Offenberg, J., and Edney, E.: Hydroxydicarboxylic Acids: Markers for Secondary Organic Aerosol from the Photooxidation of α-Pinene, Environ. Sci. Technol., 41, 1628–1634, 2007.

Conen, F., Rodríguez, S., Hüglin, C., Henne, S., Herrmann, E., Bukowiecki, N., and Alewell, C.: Atmospheric ice nuclei at the high-altitude observatory Jungfraujoch, Switzerland, Tellus, Ser. B, 67, 1–10, doi:10.3402/tellusb.v67.25014, 2015.

Cong, Z., Kang, S., Kawamura, K., Liu, B., Wan, X., Wang, Z., Gao, S. and Fu, P.: Carbonaceous aerosols on the south edge of the Tibetan Plateau: concentrations, seasonality and sources, Atmos. Chem. Phys., 15(3), 1573–1584, doi:10.5194/acp-15-1573-2015, 2015.

Cuesta, J., Marsham, J. H., Parker, D. J., and Flamant, C.: Dynamical mechanisms controlling the vertical redistribution of dust and the thermodynamic structure of the West Saharan atmospheric boundary layer during summer, Atmos. Sci. Lett., 10, 34–42, doi:10.1002/asl.207, 2009.

Draxler, R. R., and Hess, G. D.: Description of the HYSPLIT 4 modeling system. NOAA Tech.Memo. ERL ARL-224, NOAA Air Resources Laboratory, Silver Spring, MD, 1997.

Draxler, R.R. and Rolph, G.D., 2003. HYSPLIT (HYbrid Single-Particle Lagrangian Integrated Trajectory) Model access via NOAA ARL READY Website (http://www.arl.noaa.gov/ready/hysplit4.html). NOAA Air Resources Laboratory, Silver Spring, MD.

Dzepina, K., Mazzoleni, C., Fialho, P., China, S., Zhang, B., Owen, R. C., Helmig, D., Hueber, J., Kumar, S., Perlinger, J. A., Kramer, L. J., Dziobak, M. P., Ampadu, M. T., Olsen, S., Wuebbles, D. J. and Mazzoleni, L. R.: Molecular characterization of free tropospheric aerosol collected at the Pico Mountain Observatory: a case study with a long-range transported biomass burning plume, Atmos. Chem. Phys., 15(9), 5047–5068, doi:10.5194/acp-15-5047-2015, 2015.

El Haddad, I., Marchand, N., Temime-Roussel, B., Wortham, H., Piot, C., Besombes, J.-L., Baduel, C., Voisin, D., Armengaud, A., and Jaffrezo, J.-L.: Insights into the secondary fraction of the organic aerosol in a Mediterranean urban area: Marseille, Atmos. Chem. Phys., 11, 2059–2079, doi:10.5194/acp-11-2059-2011, 2011.

Fischer, H., Nikitas, C., Parchatka, U., Zenker, T., Harris, G. W., Matuska, P., Schmitt, R., Mihelcic, D., Muesgen, P., Paetz, H.-W., Schultz, M. and Volz-Thomas, A.: Trace gas measurements during the Oxidizing Capacity of the Tropospheric Atmosphere campaign 1993 at Izaña, J. Geophys. Res., 103(D11), 13505, doi:10.1029/97JD01497, 1998.

Fontal, M., van Drooge, B. L., Lopez, J. F., Fernández, P., and Grimalt, J. O.: Broad spectrum analysis of polar and apolar organic compounds in submicron atmospheric particles, J. Chromatogr. A, 1404, 28–38, 2015.

Fraser, M. P. and Lakshmanan, K.: Using levoglucosan as a molecular marker for the long-range transport of biomass combustion aerosols, Environ. Sci. Technol., 34 (21), 4560–4564, doi:10.1021/es991229l, 2000.

Frenklach, M.: Reaction mechanism of soot formation in flames, Phys. Chem. Chem. Phys., 4(11), 2028–2037, doi:10.1039/b110045a, 2002.

Fu, P., Kawamura, K., Okuzawa, K., Aggarwal, S. G., Wang, G., Kanaya, Y. and Wang, Z.: Organic molecular compositions and temporal variations of summertime mountain aerosols over Mt. Tai, North China Plain, J. Geophys. Res., 113(D19), D19107, doi:10.1029/2008JD009900, 2008.

Fu, P. Q., Kawamura, K., Pavuluri, C. M., Swaminathan, T. and Chen, J.: Molecular characterization of urban organic aerosol in tropical India: contributions of primary emissions and secondary photooxidation, Atmos. Chem. Phys., 10(6), 2663–2689, doi:10.5194/acp-10-2663-2010, 2010.

Fu, P., Kawamura, K., Kobayashi, M. and Simoneit, B. R. T.: Seasonal variations of sugars in atmospheric particulate matter from Gosan, Jeju Island: Significant contributions of airborne pollen and Asian dust in spring, Atmos. Environ., 55, 234–239, doi:10.1016/j.atmosenv.2012.02.061, 2012.

Fu, P. Q., Kawamura, K., Cheng, Y. F., Hatakeyama, S., Takami, A., Li, H. and Wang, W.: Aircraft measurements of polar organic tracer compounds in tropospheric particles (PM_{10}) over central China, Atmos. Chem. Phys., 14(8), 4185–4199, doi:10.5194/acp-14-4185-2014, 2014.

Gao, S., Hegg, D. A., Hobbs, P. V, Kirchstetter, T. W., Magi, B. I. and Sadilek, M.: Water-soluble organic components in aerosols associated with savanna fires in southern Africa: Identification, evolution, and distribution, J. Geophys. Res. Atmos., 108(D13), n/a–n/a, doi:10.1029/2002JD002324, 2003.

García, M. I., Rodríguez, S., González, Y. and García, R. D.: Climatology of new particle formation at Izaña mountain GAW observatory in the subtropical North Atlantic, Atmos. Chem. Phys., 14(8), 3865–3881, doi:10.5194/acp-14-3865-2014, 2014.

Garrison, V. H., Majewski, M. S., Foreman, W. T., Genualdi, S. A., Mohammed, A., and Massey Simonich, S. L.: Persistent organic contaminants in Saharan dust air masses in West Africa, Cape Verde and the eastern Caribbean, Sci. Total Environ., 468–469, 530–543, 2013.

Gouw, J. D. E. and Jimenez, J. L.: Organic Aerosols in the Earth's Atmosphere, , 43(20), 7614–7618, 2009.

Graham, B., Guyon, P., Taylor, P. E., Artaxo, P., Maenhaut, W., Glovsky, M. M., Flagan, R. C., and Andreae, M. O.: Organic compounds present in the natural Amazonian aerosol: characterization by gas chromatography-mass spectrometry, J. Geophys. Res., 108(D24), 4766, doi:10.1029/2003JD003990, 2003.

Griffin, D.: Atmospheric movement of microorganisms in clouds of desert dust and implications for human health, Clin. Microbiol. Rev., 20, 459–477, doi:10.1128/CMR.00039-06, 2007.

Guenther, A., Hewitt, C. N., Erickson, D., Fall, R., Geron, C.,Graedel, T., Harley, P., Klinger, L., Lerdau, M., Mckay, W. A., Pierce, T., Scholes, B., Steinbrecher, R., Tallamraju, R., Taylor, J., and Zimmerman, P.: A global-model of natural volatile organic-compound emissions, J. Geophys. Res., 100, 8873–8892, 1995.

Guenther, A. B., Jiang, X., Heald, C. L., Sakulyanontvittaya, T., Duhl, T., Emmons, L. K., and Wang, X.: The Model of Emissions of Gases and Aerosols from Nature version 2.1 (MEGAN2.1): an extended and updated framework for modeling biogenic emissions, Geosci. Model Dev., 5, 1471–1492, doi:10.5194/gmd-5-1471-2012, 2012.

Guenther, A., Karl, T., Harley, P., Wiedinmyer, C., Palmer, P. I., and Geron, C.: Estimates of global terrestrial isoprene emissions using MEGAN (Model of Emissions of Gases and Aerosols from Nature), Atmos. Chem. Phys., 6, 3181-3210, doi:10.5194/acp-6-3181-2006, 2006.

Hallquist, M., Wenger, J. C., Baltensperger, U., Rudich, Y., Simpson, D., Claeys, M., Dommen, J., Donahue, N. M., George, C., Goldstein, a. H., Hamilton, J. F., Herrmann, H., Hoffmann, T., Iinuma, Y., Jang, M., Jenkin, M. E., Jimenez, J. L., Kiendler-Scharr, A., Maenhaut, W., McFiggans, G., Mentel, T. F., Monod, A., Prévôt, a. S. H., Seinfeld, J. H., Surratt, J. D., Szmigielski, R. and Wildt, J.: The formation, properties and impact of secondary organic aerosol: current and emerging issues, Atmos. Chem. Phys., 9(14), 5155–5236, doi:10.5194/acp-9-5155-2009, 2009.

Heald, C. L., Jacob, D. J., Park, R. J., Russell, L. M., Huebert, B. J., Seinfeld, J. H., Liao, H. and Weber, R. J.: A large organic aerosol source in the free troposphere missing from current models, Geophys. Res. Lett., 32(18), 1–4, doi:10.1029/2005GL023831, 2005.

Hennigan, C. J., Sullivan, A. P., Collett, J. L. and Robinson, A. L.: Levoglucosan stability in biomass burning particles exposed to hydroxyl radicals, Geophys. Res. Lett., 37(9), n/a–n/a, doi:10.1029/2010GL043088, 2010.

Hoffmann, D.; Tilgner, A.; Iinuma, Y.; Herrmann, H. Atmospheric Stability of Levoglucosan: A Detailed Laboratory and Modeling Study. Environ. Sci. Technol. 44, 694-699, 2010.

Howsam, M. and Jones, K.: Sources of PAHs in the environment, Handb. Environ. Chem., 3, 137–174, doi:10.1007/978-3-540-49697-7_4, 1998.

Hoyle, C. R., Berntsen, T., Myhre, G., and Isaksen, I. S. A.: Secondary organic aerosol in the global aerosol – chemical transport model Oslo CTM2, Atmos. Chem. Phys., 7, 5675–5694, doi:10.5194/acp-7-5675-2007, 2007.

Hoyle, C. R., Boy, M., Donahue, N. M., Fry, J. L., Glasius, M., Guenther, A., Hallar, A. G., Huff Hartz, K., Petters, M. D., Petäjä, T., Rosenoern, T., and Sullivan, A. P.: A review of the anthropogenic influence on biogenic secondary organic aerosol, Atmos. Chem. Phys., 11, 321-343, doi:10.5194/acp-11-321-2011, 2011.

Horowitz, L. W., Liang, J., Gardner, G. M., and Jacob, D. J.: Export of reactive nitrogen from North America during summertime: Sensitivity to hydrocarbon chemistry, J. Geophys. Res.-Atmos., 103, 13451–13476, 1998.

Iinuma, Y., Brüggemann, E., Gnauk, T., Müller, K., Andreae, M. O., Helas, G., Parmar, R. and Herrmann, H.: Source characterization of biomass burning particles: The combustion of selected European conifers, African hardwood, savanna grass, and German and Indonesian peat, J. Geophys. Res., 112(D8), D08209, doi:10.1029/2006JD007120, 2007.

IPCC, 2013: Climate change 2013: The physical science basis. Contribution of Working Group I to the Fifth Assessment Report of the Intergovernmental Panel on Climate edited by: Stocker, T.F., Qin, D., Plattner, G.K. Tignor, M. , Allen, S.K. , Boschung, J. , Nauels, A. , Xia, Y. , Bex V. , and Midgley P.M. Cambridge University Press, Cambridge, UK and New York, NY, USA, 1535 pp.

Ion, A. C., Vermeylen, R., Kourtchev, I., Cafmeyer, J., Chi, X., Gelencsér, A., Maenhaut, W. and Claeys, M.: Polar organic compounds in rural $PM_{2.5}$ aerosols from K-puszta, Hungary, during a 2003 summer field campaign: Sources and diel variations, Atmos. Chem. Phys., 5(7), 1805–1814, doi:10.5194/acp-5-1805-2005, 2005.

Izquierdo, R., Belmonte, J., Avila, A., Alarcón, M., Cuevas, E., and Alonso-Pérez, S.: Source areas and long-range transport of pollen from continental land to Tenerife (Canary Islands), Int. J. Biometeorol., 55, 67–85, doi: 10.1007/s00484-010-0309-1, 2011.

Jang, M. and Mcdow, S. R.: Products of benz[a]anthracene photodegradation in the presence of known organic constituents of atmospheric aerosols, Environ. Sci. Technol., 31(4), 1046–1053, doi:10.1021/es960559s, 1997.

Jaumot, J., Gargallo, R., de Juan, A. and Tauler, R.: A graphical user-friendly interface for MCR-ALS: a new tool for multivariate curve resolution in MATLAB, Chemom. Intell. Lab. Syst., 76(1), 101–110, doi:10.1016/j.chemolab.2004.12.007, 2005.

Kanakidou, M., Seinfeld, J. H., Pandis, S. N., Barnes, I., Dentener, F. J., Facchini, M. C., Van Dingenen, R., Ervens, B., Nenes, A., Nielsen, C. J., Swietlicki, E., Putaud, J. P., Balkanski, Y., Fuzzi, S., Horth, J., Moortgat, G. K., Winterhalter, R., Myhre, C. E. L., Tsigaridis, K., Vignati, E., Stephanou, E. G., and Wilson, J.: Organic aerosol and global climate modelling: a review, Atmos. Chem. Phys., 5, 1053-1123, doi:10.5194/acp-5-1053-2005, 2005.

Karanasiou, A., Minguillón, M. C., Viana, M., Alastuey, A., Putaud, J.-P., Maenhaut, W., Panteliadis, P., Močnik, G., Favez, O., and Kuhlbusch, T. A. J.: Thermal-optical analysis for the measurement of elemental carbon (EC) and organic carbon (OC) in ambient air a literature review, Atmos. Meas. Tech. Discuss., 8, 9649-9712, doi:10.5194/amtd-8-9649-2015, 2015.

Kawamura, K. and Kaplan, I. R.: Motor Exhaust Emissions as a Primary Source for Dicarboxylic Acids in Los Angeles Ambient Air, Environ. Sci. Technol., 21(1), 105–110, doi:10.1021/es00155a014, 1987.

Kawamura, K. and Sakaguchi, F.: Molecular distributions of water soluble dicarboxylic acids in marine aerosols over the Pacific Ocean including tropics, J. Geophys. Res. Atmos., 104, 3501–3509, 1999.

Kirchstetter, T. Novakov, W., T., and Hobbs, P. V.: Evidence that the spectral dependence of light absorption by aerosols is affected by organic carbon. J. Geophys. Res., 109, D21208, doi:10.1029/2004JD004999, 2004.

Kleindienst, T. E., Jaoui, M., Lewandowski, M., Offenberg, J. H. and Docherty, K. S.: The formation of SOA and chemical tracer compounds from the photooxidation of naphthalene and its methyl analogs in the presence and absence of nitrogen oxides, Atmos. Chem. Phys., 12(18), 8711–8726, doi:10.5194/acp-12-8711-2012, 2012.

Kroll, J. H., Ng, N. L., Murphy, S. M., Flagan, R. C., and Seinfeld, J. H.: Secondary organic aerosol formation from isoprene photooxidation, Environ. Sci. Technol., 40, 1869–1877, 2006.

Lamarque, J.-F., Bond, T. C., Eyring, V., Granier, C., Heil, A., Klimont, Z., Lee, D., Liousse, C., Mieville, A., Owen, B., Schultz, M. G., Shindell, D., Smith, S. J., Stehfest, E., Van Aardenne, J., Cooper, O. R., Kainuma, M., Mahowald, N., McConnell, J. R., Naik, V., Riahi, K. and van Vuuren, D. P.: Historical (1850–2000) gridded anthropogenic and

biomass burning emissions of reactive gases and aerosols: methodology and application, Atmos. Chem. Phys., 10(15), 7017–7039, doi:10.5194/acp-10-7017-2010, 2010.

Luo, G. and Yu, F.: A numerical evaluation of global oceanic emissions of α-pinene and isoprene, Atmos. Chem. Phys., 10, 2007-2015, doi:10.5194/acp-10-2007-2010, 2010.

Mao, J., Paulot, F., Jacob, D. J., Cohen, R. C., Crounse, J. D., Wennberg, P. O., Keller, C. A., Hudman, R. C., Barkley, M. P., and Horowitz, L. W.: Ozone and organic nitrates over the eastern United States: Sensitivity to isoprene chemistry, J. Geophys. Res.-Atmos., 118, 11256–11268, doi:10.1002/jgrd.50817, 2013.

Marais, E. A., Jacob, D. J., Jimenez, J. L., Campuzano-Jost, P., Day, D. A., Hu, W., Krechmer, J., Zhu, L., Kim, P. S., Miller, C. C., Fisher, J. A., Travis, K., Yu, K., Hanisco, T. F., Wolfe, G. M., Arkinson, H. L., Pye, H. O. T., Froyd, K. D., Liao, J., and McNeill, V. F.: Aqueous-phase mechanism for secondary organic aerosol formation from isoprene: application to the southeast United States and co-benefit of SO2 emission controls, Atmos. Chem. Phys., 16, 1603-1618, doi:10.5194/acp-16-1603-2016, 2016.

Maring, H., Savoie, D. L., Izaguirre, M. A., McCormick, C., Arimoto, R., Prospero, J. M. and Pilinis, C.: Aerosol physical and optical properties and their relationship to aerosol composition in the free troposphere at Izaña, Tenerife, Canary Islands, during July 1995, J. Geophys. Res. Atmos., 105(D11), 14677–14700, doi:10.1029/2000JD900106, 2000.

Mazurek, M. A., Cass, G. R. and Simoneit, B. R. T.: Interpretation of High-Resolution Gas Chromatography and High-Resolution Gas Chromatography / Mass Spectrometry Data Acquired from Atmospheric Organic Aerosol Samples, Aerosol Sci. Technol., 10(2), 408–420, doi:10.1080/02786828908959280, 1989.

Medeiros, P. M. and Simoneit, B. R. T.: Analysis of sugars in environmental samples by gas chromatography-mass spectrometry, J. Chromatogr. A, 1141(2), 271–278, doi:10.1016/j.chroma.2006.12.017, 2007.

Meng, J., Wang, G., Li, J., Cheng, C., Ren, Y., Huang, Y., Cheng, Y., Cao, J., and Zhang, T.: Seasonal characteristics of oxalic acid and related SOA in the free troposphere of Mt. Hua, central China: implications for sources and formation mechanisms, Sci Total Environ, 493, 1088-1097, 2014.

Merrill, J. T., and Moody J. L.: Synoptic meteorology and transport during the North Atlantic Regional Experiment (NARE) intensive: Overview, J. Geophys. Res., 101, 28, 903–28,921, 1996.

Mochida, M., Kawamura, K., Umemoto, N., Kobayashi, M., Matsunaga, S., Lim, H. J., Turpin, B. J., Bates, T. S. and Simoneit, B. R. T.: Spatial distributions of oxygenated organic compounds (dicarboxylic acids, fatty acids, and levoglucosan) in marine aerosols over the western Pacific and off the coast of East Asia: Continental outflow of organic aerosols during the ACE-Asia campaign, J. Geophys. Res., 108(D23), 8638, doi:doi:10.1029/2002JD003249, 2003.

Moise, T. and Rudich, Y.: Reactive Uptake of Ozone by Aerosol-Associated Unsaturated Fatty Acids: Kinetics, Mechanism, and Products, J. Phys. Chem. A, 106, 669-6476, 2002.

Narukawa, M., Kawamura, K., Takeuchi, N., and Nakajima, T.: Distribution of dicarboxylic acids and carbon isotopic compositions in aerosols from 1997 Indonesian forest fires, Geophys. Res. Lett., 26, 3101–3104, 1999.

Ng, N. L., Chhabra, P. S., Chan, A. W. H., Surratt, J. D., Kroll, J. H., Kwan, A. J., McCabe, D. C., Wennberg, P. O., Sorooshian, A., Murphy, S. M., Dalleska, N. F., Flagan, R. C., and Seinfeld, J. H.: Effect of NOx level on secondary organic aerosol (SOA) formation from the photooxidation of terpenes, Atmos. Chem. Phys., 7, 5159–5174, doi:10.5194/acp-7-5159-2007, 2007.

Ng, N. L., Kwan, A. J., Surratt, J. D., Chan, A. W. H., Chhabra, P. S., Sorooshian, A., Pye, H. O. T., Crounse, J. D., Wennberg, P. O., Flagan, R. C., and Seinfeld, J. H.: Secondary organic aerosol (SOA) formation from reaction of isoprene with nitrate radicals (NO_3), Atmos. Chem. Phys., 8, 4117–4140, doi:10.5194/acp-8- 4117-2008, 2008.

Ng, N. L., Brown, S. S., Archibald, A. T., Atlas, E., Cohen, R. C., Crowley, J. N., Day, D. A., Donahue, N. M., Fry, J. L., Fuchs, H., Griffin, R. J., Guzman, M. I., Herrmann, H., Hodzic, A., Iinuma, Y., Jimenez, J. L., Kiendler-Scharr, A., Lee, B. H., Luecken, D. J., Mao, J., McLaren, R., Mutzel, A., Osthoff, H. D., Ouyang, B., Picquet-Varrault, B., Platt, U., Pye, H. O. T., Rudich, Y., Schwantes, R. H., Shiraiwa, M., Stutz, J., Thornton, J. A., Tilgner, A., Williams, B. J., and Zaveri, R. A.: Nitrate radicals and biogenic volatile organic compounds: oxidation, mechanisms, and organic aerosol, Atmos. Chem. Phys., 17, 2103-2162, doi:10.5194/acp-17-2103-2017, 2017.

O'Brien, J., Shepson, P., Muthuramu, K., Hao, C., Niki, H., Hastie, D., Taylor, R., and Roussel, P.: Measurements of alkyl and multifunctional organic nitrates at a rural site in Ontario, J. Geophys. Res., 100, 22795–22804, 1995.

Paulot, F., Crounse, J. D., Kjaergaard, H. G., Kroll, J. H., Seinfeld, J. H., and Wennberg, P. O.: Isoprene photooxidation: new insights into the production of acids and organic nitrates, Atmos. Chem. Phys., 9, 1479–1501, doi:10.5194/acp-9-1479-2009, 2009a.

Paulot, F., Crounse, J. D., Kjaergaard, H. G., Kürten, A., St Clair, J. M., Seinfeld, J. H., and Wennberg, P. O.: Unexpected epoxideformation in the gas-phase photooxidation of isoprene, Science, 325, 730–733, doi:10.1126/science.1172910, 2009b.

Paulot, F., Wunch, D., Crounse, J. D., Toon, G. C., Millet, D. B., Decarlo, P. F., Vigouroux, C., Deutscher, N. M., Abad, G. G., Notholt, J., Warneke, T., Hannigan, J. W., Warneke, C., De Gouw, J. A., Dunlea, E. J., De Mazière, M., Griffith, D. W. T., Bernath, P., Jimenez, J. L. and Wennberg, P. O.: Importance of secondary sources in the atmospheric budgets of formic and acetic acids, Atmos. Chem. Phys., 11(5), 1989–2013, doi:10.5194/acp-11-1989-2011, 2011.

Pérez García-Pando, C., R. L. Miller, J. P. Perlwitz, S. Rodríguez, and Prospero, J. M.: Predicting the mineral composition of dust aerosols: Insights from elemental composition measured at the Izaña Observatory. Geophys. Res. Lett., 43, 19, 10520-10529, doi:10.1002/2016GL069873, 2016.

Pitchford, M., Maim, W., Schichtel, B., Kumar, N., Lowenthal, D. and Hand, J.: Revised algorithm for estimating light extinction from IMPROVE particle speciation data., J. Air Waste Manag. Assoc., 57(January 2015), 1326–1336, doi:10.3155/1047-3289.57.11.1326, 2007.

Presto, A. A., Hartz, K. E. H., and Donahue, N. M.: Secondary organic aerosol production from terpene ozonolysis. 2. Effect of NOx concentration, Environ. Sci. Technol., 39, 7046–7054, doi: 10.1021/Es050400s, 2005.

Prospero, J. M. and Carlson, T. N.: Vertical and areal distribution of Saharan dust over the western Equatorial North Atlantic Ocean, J. Geophys. Res., 77, 5255–5265, 1972.

Puxbaum, H., Caseiro, A., Sánchez-Ochoa, A., Kasper-Giebl, A., Cleays, M., Gelencsér, A., Legrand, M., Preunkert, S., and Pio, C.: Levoglucosan levels at background sites in Europe for assessing the impact of biomass combustion on the European aerosol background, J. Geophys. Res., 112, D23S05, doi:10.1029/2006JD008114, 2007.

Pye, H. O. T., Chan, A. W. H., Barkley, M. P., and Seinfeld, J. H.: Global modeling of organic aerosol: the importance of reactive nitrogen (NOx and NO3), Atmos. Chem. Phys., 10, 11261-11276, doi:10.5194/acp-10-11261-2010, 2010.

Rinne, J., Bäck, J. and Hakola, H.: Biogenic volatile organic compound emissions from the Eurasian taiga: Current knowledge and future directions, Boreal Environ. Res., 14(4), 807–826 [online] Available from: http://www.scopus.com/inward/record.url?eid=2-s2.0-69949092124&partnerID=40&md5=64765c400b7ae11f40cb879cffbc7515, 2009.

Rodríguez, S., González, Y., Cuevas, E., Ramos, R., Romero, P. M., Abreu-Afonso, J. and Redondas, A.: Atmospheric nanoparticle observations in the low free troposphere during upward orographic flows at Izaña Mountain Observatory, Atmos. Chem. Phys., 9(17), 6319–6335, doi:10.5194/acp-9-6319-2009, 2009.

Rodríguez, S., Alastuey, A., Alonso-Pérez, S., Querol, X., Cuevas, E., Abreu-Afonso, J., Viana, M., Pérez, N., Pandolfi, M. and De La Rosa, J.: Transport of desert dust mixed with North African industrial pollutants in the subtropical Saharan Air Layer, Atmos. Chem. Phys., 11(13), 6663–6685, doi:10.5194/acp-11-6663-2011, 2011.

Rodríguez, S., Cuevas, E., Prospero, J. M., Alastuey, A., Querol, X., López-Solano, J., García, M. I. and Alonso-Pérez, S.: Modulation of Saharan dust export by the North African dipole, Atmos. Chem. Phys., 15(13), 7471–7486, doi:10.5194/acp-15-7471-2015, 2015.

Rogge, W. F., Hildemann, L. M., Mazurek, M. a., Cass, G. R. and Simoneit, B. R. T.: Sources of fine organic aerosol. 2. Noncatalyst and catalyst-equipped automobiles and heavy-duty diesel trucks, Environ. Sci. Technol., 27(4), 636–651, doi:10.1021/es00041a007, 1993.

Salisbury, G.; Williams, J.; Gros, V.; Bartenbach, S.; Xu, X.; Fischer, H.; Kormann, R.; de Reus, M.; Zoellner, M.: Assessing the effect of a Saharan dust storm on oxygenated organic compounds at Izana, Tenerife (July–August 2002), J. Geophys. Res. Atmos, 111, , D2230, doi:10.1029/2005JD006840, 2006.

Saxton, J. E., Lewis, A. C., Kettlewell, J. H., Ozel, M. Z., Gogus, F., Boni, Y., Korogone, S. O. U. and Serca, D.: Isoprene and monoterpene measurements in a secondary forest in northern Benin, Atmos. Chem. Phys., 7(15), 4095–4106, doi:10.5194/acp-7-4095-2007, 2007.

Schauer, J., Rogge, W., Hildemann, L., Mazurek, M., Cass, G. and Simoneit, B.: Source apportionment of airborne particulate matter using organic compounds as tracers, Atmos. Environ., 41, 241–259, doi:10.1016/j.atmosenv.2007.10.069, 1996.

Schauer, J. J., Kleeman, M. J., Cass, G. R. and Simoneit, B. R. T.: Measurement of emissions from air pollution sources. 5. C1-C32 organic compounds from gasoline-powered motor vehicles., Environ. Sci. Technol., 36(6), 1169–1180, doi:10.1021/es0108077, 2002.

Simoneit, B. R. T.: Organic matter in eolian dusts over the Atlantic Ocean, Mar. Chem., 5, 443–464, 1977.

Simoneit, B. R. T., Sheng, G., Chen, X., Fu, J., Zhang, J. and Xu, Y.: Molecular marker study of extractable organic matter in aerosols from urban areas of China, Atmos. Environ. Part A, Gen. Top., 25(10), 2111–2129, doi:10.1016/0960-1686(91)90088-O, 1991.

Simoneit, B. R. T.: Biomass burning - A review of organic tracers for smoke from incomplete combustion, Appl. Geochemistry, 17(3), 129–162, doi:10.1016/S0883-2927(01)00061-0, 2002.

Simoneit, B. R. T., Elias, V. O., Kobayashi, M., Kawamura, K., Rushdi, A. I., Medeiros, P. M., Rogge, W. F. and Didyk, B. M.: Sugars: dominant water-soluble organic compounds in soils and characterization as tracers in atmospheric particulate matter., Environ. Sci. Technol., 38(22), 5939–5949, doi:10.1021/es0403099, 2004a.

Simoneit, B. R. T., Kobayashi, M., Mochida, M., Kawamura, K. and Huebert, B. J.: Aerosol particles collected on aircraft flights over the northwestern Pacific region during the ACE-Asia campaign: Composition and major sources of the organic compounds, J. Geophys. Res. D Atmos., 109(19), D19S09, doi:10.1029/2004JD004565, 2004b.

Sindelarova, K., Granier, C., Bouarar, I., Guenther, A., Tilmes, S., Stavrakou, T., Müller, J.-F., Kuhn, U., Stefani, P., and Knorr, W.: Global data set of biogenic VOC emissions calculated by the MEGAN model over the last 30 years, Atmos. Chem. Phys., 14, 9317-9341, doi:10.5194/acp-14-9317-2014, 2014.

Smolander, S., He, Q., Mogensen, D., Zhou, L., Bäck, J., Ruuskanen, T., Noe, S., Guenther, A., Aaltonen, H., Kulmala, M. and Boy, M.: Comparing three vegetation monoterpene emission models to measured gas concentrations with a model of meteorology, air chemistry and chemical transport, Biogeosciences, 11(19), 5425–5443, doi:10.5194/bg-11-5425-2014, 2014.

Stein, A. F., Draxler, R. R., Rolph, G. D., Stunder, B. J. B., Cohen, M. D. and Ngan, F.: NOAA's HYSPLIT Atmospheric Transport and Dispersion Modeling System, Bull. Am. Meteorol. Soc., 96(12), 2059–2077, doi:10.1175/BAMS-D-14-00110.1, 2015.

Sun, J., and Ariya, P. A.: Atmospheric organic and bio-aerosols as cloud condensation nuclei (CCN): A review, Atmos. Environ., 40, 795-820,doi: 10.1016/j.atmosenv.2005.05.052, 2006.

Surratt, J. D., Murphy, S. M., Kroll, J. H., Ng, N. L., Hildebrandt, L., Sorooshian, A., Szmigielski, R., Vermeylen, R., Maenhaut, W., Claeys, M., Flagan, R. C., and Seinfeld, J. H.: Chemical Composition of Secondary Organic Aerosol Formed from the Photooxidation of Isoprene, J. Phys. Chem. A, 110, 9665–9690, doi:10.1021/jp061734m, 2006.

Surratt, J. D., Lewandowski, M., Offenberg, J. H., Jaoui, M., Kleindienst, T. E., Edney, E. O. and Seinfeld, J. H.: Effect of acidity on secondary organic aerosol formation from isoprene, Environ. Sci. Technol., 41(15), 5363–5369, doi:10.1021/es0704176, 2007.

Szmigielski, R., Surratt, J. D., Gómez-González, Y., Van der Veken, P., Kourtchev, I., Vermeylen, R., Blockhuys, F., Jaoui, M., Kleindienst, T. E., Lewandowski, M., Offenberg, J. H., Edney, E. O., Seinfeld, J. H., Maenhaut, W., and Claeys, M.: 3-Methyl-1,2,3-butanetricarboxylic acid: an atmospheric tracer for terpene secondary organic aerosol, Geophys. Res. Lett., 34, L24811, doi:10.1029/2007GL031338, 2007.

Tauler, R.: Multivariate curve resolution applied to second order data, Chemometr. Intell. Lab., 30, 133–146, 1995a.

Tauler, R., Smilde, A., and Kowalski, B.: Selectivity, local rank, 3-way data-analysis and ambiguity in multivariate curve resolution,J. Chemometr., 9, 31–58, 1995b.

Tauler, R., Viana, M., Querol, X., Alastuey, A., Flight, R. M., Wentzell, P. D. and Hopke, P. K.: Comparison of the results obtained by four receptor modelling methods in aerosol source apportionment studies, Atmos. Environ., 43(26), 3989–3997, doi:10.1016/j.atmosenv.2009.05.018, 2009.

Tsamalis, C., Chédin, A., Pelon, J., and Capelle, V.: The seasonal vertical distribution of the Saharan Air Layer and its modulation by the wind, Atmos. Chem. Phys., 13, 11235–11257, doi:10.5194/acp-13-11235-2013, 2013.

Van Drooge, B. L., Fernández, P., Grimalt, J. O., Stuchlík, E., Torres García, C. J. and Cuevas, E.: Atmospheric polycyclic aromatic hydrocarbons in remote European and Atlantic sites located above the boundary mixing layer., Environ. Sci. Pollut. Res. Int., 17(6), 1207–16, doi:10.1007/s11356-010-0296-0, 2010.

Van Drooge, B.L., Grimalt, J.O.: Particle size-resolved source apportionment of primary and secondary organic tracer compounds at urban and rural locations in Spain, Atmos. Chem. Phys., 15, 7735–7752, 2015.

Volkamer, R., Jimenez, J. L., San Martini, F., Dzepina, K., Zhang, Q., Salcedo, D., Molina, L. T., Worsnop, D. R., and Molina, M. J.: Secondary organic aerosol formation from anthropogenic air pollution: rapid and higher than expected, Geophys. es. Lett., 33, L17811, doi:10.1029/2006GL026899, 2006.

Von Schneidemesser, E., Schauer, J. J., Hagler, G. S. W. and Bergin, M. H.: Concentrations and sources of carbonaceous aerosol in the atmosphere of Summit, Greenland, Atmos. Environ., 43(27), 4155–4162, doi:10.1016/j.atmosenv.2009.05.043, 2009.

Wang, G. H., Kawamura, K., Umemoto, N., Xie, M. J., Hu, S. Y., and Wang, Z. F.: Water-soluble organic compounds in $PM_{2.5}$ and size-segregated aerosols over Mount Tai in North China Plain, J. Geophys. Res.-Atmos., 114, D19208, doi:10.1029/2008JD011390 , 2009.

Winker, D. M., Tackett, J. L., Getzewich, B. J., Liu, Z., Vaughan, M. A., and Rogers, R. R.: The global 3-D distribution of tropospheric aerosols as characterized by CALIOP, Atmos. Chem. Phys., 13, 3345-3361, doi:10.5194/acp-13-3345-2013, 2013.

Xu, J. Z., Zhang, Q., Wang, Z. B., Yu, G. M., Ge, X. L. and Qin, X.: Chemical composition and size distribution of summertime $PM_{2.5}$ at a high altitude remote location in the northeast of the Qinghai-Xizang (Tibet) Plateau: Insights into aerosol sources and processing in free troposphere, Atmos. Chem. Phys., 15(9), 5069–5081, doi:10.5194/acp-15-5069-2015, 2015.

Yan, F., Winijkul, E., Streets, D. G., Lu, Z., Bond, T. C., and Zhang, Y.: Global emission projections for the transportation sector using dynamic technology modeling, Atmos. Chem. Phys., 14, 5709-5733, doi:10.5194/acp-14-5709-2014, 2014.

Yttri, K. E., Dye, C. and Kiss, G.: Ambient aerosol concentrations of sugars and sugar-alcohols at four different sites in Norway, Atmos. Chem. Phys. Discuss., 7(2), 5769–5803, doi:10.5194/acpd-7-5769-2007, 2007.

Table 1. Average concentration of the chemical major compounds for (i) FT-PM_T and BL-$PM_{2.5}$ having into account all samples, (ii) FT-PM_T and BL-$PM_{2.5}$ collected within the Saharan air layer (SAL) , (iii) FT-PM_T and BL-$PM_{2.5}$ collected within the Westerlies (WES) without the FT-PM_T biomass burning event and (iv) FT-PM_T biomass burning event (BBE).

	FT-PM_T ALL	**BL-$PM_{2.5}$ ALL**	**FT-PM_T SAL**	**FT-PM_T WES**	**BL-$PM_{2.5}$ SAL**	**BL-$PM_{2.5}$ WES**	**FT-PM_T BBE**
$\sum$ CC, $\mu g \cdot m^{-3}$	78.98	13.70	92.74	2.16	17.07	4.70	6.84
Dust, $\mu g \cdot m^{-3}$	73.61	11.18	86.71	1.51	14.10	3.39	1.66
Sea Salt, $\mu g \cdot m^{-3}$	0.53	0.36	0.59	0.27	0.25	0.66	< 0.01
OM, $\mu g \cdot m^{-3}$	1.32	0.47	1.39	0.04	0.61	0.09	3.64
EC, $\mu g \cdot m^{-3}$	0.04	0.07	0.03	< 0.01	0.08	0.05	0.29
NO_3^-, $\mu g \cdot m^{-3}$	0.73	0.08	0.87	< 0.01	0.11	< 0.01	< 0.01
NH_4^+, $\mu g \cdot m^{-3}$	0.33	0.25	0.35	0.14	0.32	0.07	0.54
nss-$SO_4^=$, $\mu g \cdot m^{-3}$	2.42	1.28	2.80	0.19	1.61	0.43	0.71
ss-$SO_4^=$, $\mu g \cdot m^{-3}$	0.02	0.01	0.02	0.01	0.01	0.03	< 0.01

$\sum$**CC**: sum chemical composition; **OM**: organic matter; **EC**: elemental carbon; **nss-$SO_4^=$**: non sea salt sulphate; **ss-$SO_4^=$**: sea salt sulphate.

Table 2. Average concentration of the selected organic species for (i) FT-PM_T and BL-$PM_{2.5}$ having into account all samples, (ii) FT-PM_T and BL-$PM_{2.5}$ collected within the Saharan air layer (SAL), (iii) FT-PM_T and BL-$PM_{2.5}$ collected within the Westerlies (WES) without the FT-PM_T biomass burning event and (iv) FT-PM_T biomass burning event (BBE).

	FT-PM_T ALL	BL-$PM_{2.5}$ ALL	FT-PM_T SAL	FT-PM_T WES	BL-$PM_{2.5}$ SAL	BL-$PM_{2.5}$ WES	FT-PM_T BBE
Levoglucosan							
Levoglucosan, ng·m^{-3}	0.75	0.53	0.41	0.40	0.34	1.04	9.33
Dicarboxylic acids							
Succinic, ng·m^{-3}	6.51	3.70	5.70	3.52	4.03	2.80	33.35
Glutaric, ng·m^{-3}	1.97	0.83	1.90	0.74	0.85	0.77	7.23
Adipic, ng·m^{-3}	1.43	0.69	1.53	0.62	0.72	0.60	1.71
Pimelic, ng·m^{-3}	0.83	0.35	0.92	0.37	0.33	0.39	0.17
Suberic, ng·m^{-3}	0.48	0.30	0.50	0.29	0.29	0.31	0.39
Azelaic, ng·m^{-3}	0.88	0.79	0.93	0.57	0.78	0.82	0.71
Malic, ng·m^{-3}	2.01	2.15	0.75	1.20	1.67	3.43	32.21
Phthalic, ng·m^{-3}	3.18	2.77	2.19	9.43	2.38	3.80	6.21
Saccharides							
α-glucose, ng·m^{-3}	9.26	0.90	10.79	0.62	0.90	0.89	1.65
β-glucose, ng·m^{-3}	9.13	1.00	10.63	0.61	1.01	0.98	1.65
Fructose, ng·m^{-3}	2.02	1.01	2.23	0.95	1.10	0.76	0.69
Sucrose, ng·m^{-3}	2.72	0.47	3.18	0.27	0.18	1.26	0.01
Mannitol, ng·m^{-3}	0.35	0.12	0.40	0.08	0.12	0.12	0.07
n-Alkanes							
nC24, ng·m^{-3}	0.72	1.63	0.75	0.48	1.87	0.97	1.01
nC25, ng·m^{-3}	0.93	2.93	0.95	0.40	3.26	2.05	2.09
nC26, ng·m^{-3}	0.60	0.64	0.65	0.26	0.69	0.49	0.54
nC27, ng·m^{-3}	0.89	0.95	0.98	0.24	0.94	0.98	0.76
nC28, ng·m^{-3}	0.37	0.32	0.39	0.17	0.38	0.17	0.36
nC29, ng·m^{-3}	1.18	0.42	1.34	0.25	0.48	0.25	0.63
nC30, ng·m^{-3}	0.45	0.14	0.51	0.07	0.16	0.10	0.18
nC31, ng·m^{-3}	1.55	0.31	1.77	0.37	0.33	0.25	0.29
nC32, ng·m^{-3}	0.39	0.10	0.45	0.05	0.11	0.06	0.08
nC33, ng·m^{-3}	0.48	0.10	0.55	0.06	0.12	0.06	0.13
nC34, ng·m^{-3}	0.29	0.05	0.34	0.02	0.05	0.04	0.01
Hopanes							
Hopane, ng·m^{-3}	0.06	0.02	0.07	0.01	0.03	0.01	0.03
nor-Hopane, ng·m^{-3}	0.07	0.05	0.08	0.02	0.07	0.02	0.03
PAHs							
B [a] A, pg·m^{-3}	1.48	1.48	1.58	0.80	1.61	1.13	1.37
Chr, pg·m^{-3}	4.27	4.37	4.63	1.92	5.12	2.39	3.38
B [b+j+k] F, pg·m^{-3}	3.67	5.74	4.20	0.66	6.69	3.21	1.13
B [e] P, pg·m^{-3}	1.36	1.94	1.50	0.47	2.22	1.20	0.83
B [a] P, pg·m^{-3}	0.78	1.21	0.89	0.18	1.25	1.08	0.29
In[123cd] P, pg·m^{-3}	1.47	2.33	1.65	0.46	2.18	2.74	0.56
B [ghi] Per, pg·m^{-3}	3.29	6.94	3.56	1.73	6.37	8.46	1.84
SOA PIN							
Cis-Pinonic, ng·m^{-3}	27.83	15.24	32.72	0.89	13.23	20.59	1.00
3-HGA, ng·m^{-3}	0.21	0.51	0.09	0.24	0.39	0.81	2.88
MBTCA, ng·m^{-3}	0.03	0.24	0.01	0.05	0.13	0.54	0.27
SOA ISO							
2MGA, ng·m^{-3}	4.22	2.38	4.46	1.63	2.65	1.65	6.56
2MT-1, ng·m^{-3}	6.64	4.94	7.27	3.40	5.16	4.33	2.40
2MT-2, ng·m^{-3}	15.45	9.53	16.79	8.95	9.24	10.31	5.53

B[a]A: benz[a]anthracene; **Chr**: chrysene; **B[b+j+k]F**: benzo[b+k]fluoranthene; **B[e]P**: benzo[e]pyrene; **B[a]P**: benzo[a]pyrene; **In[123cd]P**: indeno[1,2,3-cd]pyrene; **B[ghi]Per**: benzo[ghi]perylene; **3-HGA**: 3-hydroxyglutaric acid; **MBTCA**: 3-methyl-1,2,3-butanetricarboxylic acid; **2MGA**: 2-methylglyceric acid; **2MT-1**: 2-methylthreitol; **2MT-2**: 2-methylerythritol.

Table 3. Pearson correlation coefficients matrix of the organic and inorganic compounds within the free troposphere (PM_T). Highly statistically significant correlations (p-value < 0.01) are highlighted. BBE was excluded in this analysis.

	Levoglucosan	Dicarboxylic acids	Saccharides	n-Alkanes	Hopanes	PAHs	SOA PIN	SOA ISO	Dust	Sea Salt	OM	EC	NO_3^-	NH_4^+	nss-$SO_4^=$	ss-$SO_4^=$
Levoglucosan	1.0															
Dicarboxylic acids	0.0	1.0														
Saccharides	0.0	0.4	1.0													
n-Alkanes	0.1	0.5	**0.5**	1.0												
Hopanes	0.0	**0.6**	**0.7**	**0.8**	1.0											
PAHs	0.3	0.3	0.2	0.3	0.3	1.0										
SOA PIN	-0.1	0.2	0.3	**0.6**	0.5	0.1	1.0									
SOA ISO	0.2	0.3	0.2	0.3	0.3	**0.6**	0.4	1.0								
Dust	0.0	**0.7**	**0.6**	**0.7**	**0.9**	0.2	**0.7**	0.2	1.0							
Sea Salt	**0.6**	-0.1	-0.2	-0.1	-0.3	0.4	0.1	0.2	-0.2	1.0						
OM	-0.1	0.3	0.3	**0.7**	**0.8**	0.2	**0.8**	0.4	**0.9**	0.0	1.0					
EC	0.2	0.1	-0.1	-0.1	-0.2	**0.7**	-0.2	0.3	-0.3	0.3	-0.2	1.0				
NO_3^-	0.0	0.4	**0.7**	**0.8**	**0.8**	0.5	**0.6**	0.4	**0.8**	-0.1	**0.8**	0.0	1.0			
NH_4^+	0.1	0.1	0.2	0.2	0.3	**0.6**	-0.1	0.3	0.2	0.0	0.2	0.5	0.5	1.0		
nss-$SO_4^=$	0.1	0.2	**0.6**	0.5	**0.6**	0.5	0.5	**0.6**	0.5	0.1	**0.6**	0.1	**0.8**	**0.7**	1.0	
ss-$SO_4^=$	**0.6**	0.0	-0.2	0.0	-0.2	0.4	0.1	0.2	-0.2	**1.0**	0.0	0.3	0.0	0.0	0.0	1.0

OM: organic matter; **EC**: elemental carbon; **nss-$SO_4^=$**: non sea salt sulphate; **ss-$SO_4^=$**: sea salt sulphate.

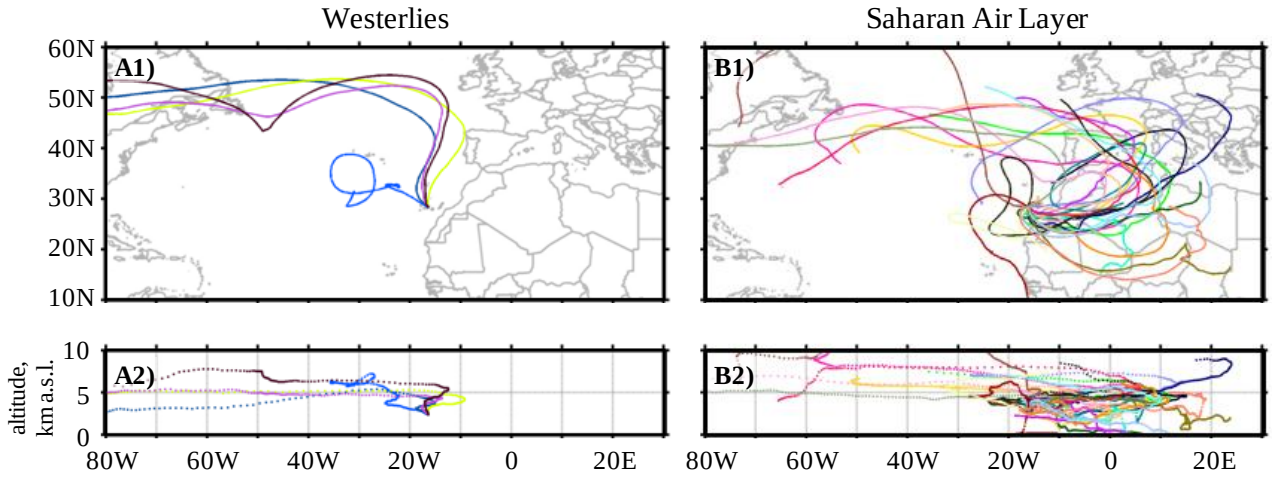

Figure 1: Ten-day back-trajectories based on HYSPLIT model for the samples collected within the **(A)** Westerlies (26Aug–30Aug) and (**B**) the Saharan Air Layer (01Aug–25Aug and 31Aug–01Sep); the dates refer to the day of completion of the sampling.

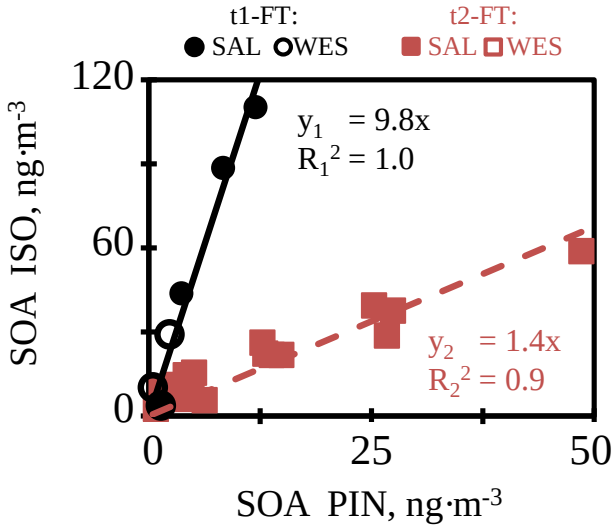

Figure 2: Scatter plot between total concentration of SOA ISO and total concentration of SOA PIN within the FT (PM_T collected during the night). Two tendencies can be distinguished: tendency-1 (t1; circles) and tendency-2 (t2; squares). Filled markers correspond to measurements within the SAL and open markers to measurements within the WES.

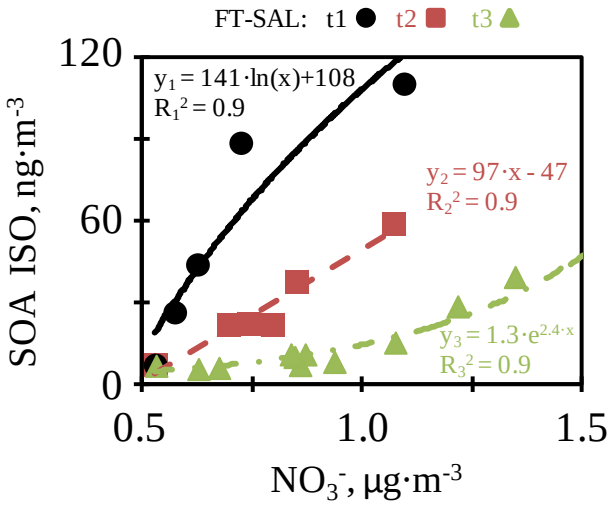

Figure 3: Scatter plot between SOA ISO and nitrate within the SAL under FT conditions (FT-PM_T samples collected during the night). Three tendencies can be distinguished: tendency-1 (t1; circles), tendency-2 (t2; squares) and tendency-3 (t3; triangles). Westerlies were excluded when calculating the regression coefficients as values were under the detection limit.

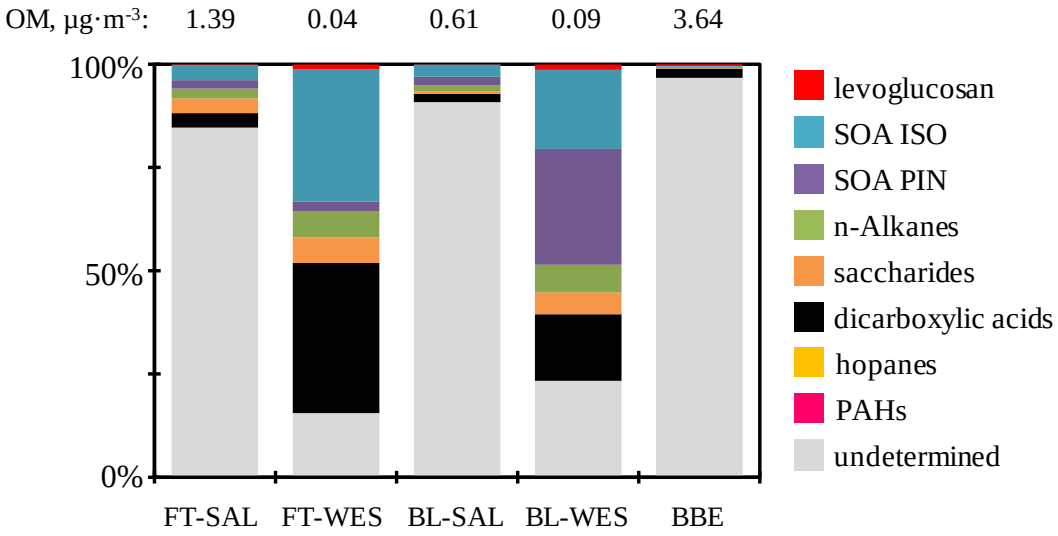

Figure 4: Contribution of the eight analysed organic groups to the Izaña OM composition within the FT and the BL under the SAL (FT-SAL and BL-SAL) and the WES (FT-WES, BL-WES, BBE). Average total OM for each air mass is on top. FT-PM_T samples were collected during the night (22–6 GMT) and BL-$PM_{2.5}$ samples were collected during the day (10–16 GMT).

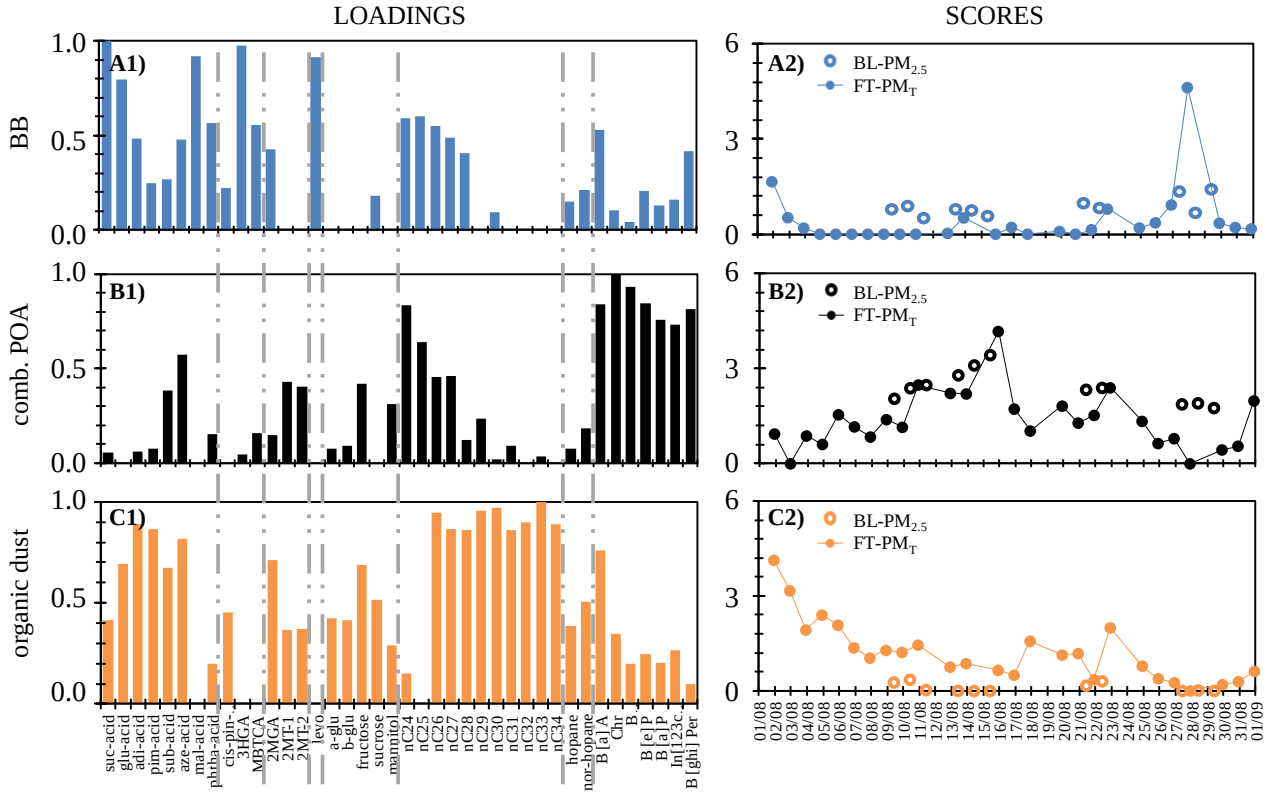

Figure 5: FT-PM_T (night) and BL-$PM_{2.5}$ (day) loadings and scores of the three components from MCR-ALS resolved profiles. Filled markers correspond to FT-PM_T and open markers to BL-$PM_{2.5}$. Grey lines separate the compounds belonging to the different organic groups: dicarboxylic acids, SOA PIN, SOA ISO, levoglucosan, saccharides, n-alkanes, hopanes and PAHs (from left to right).

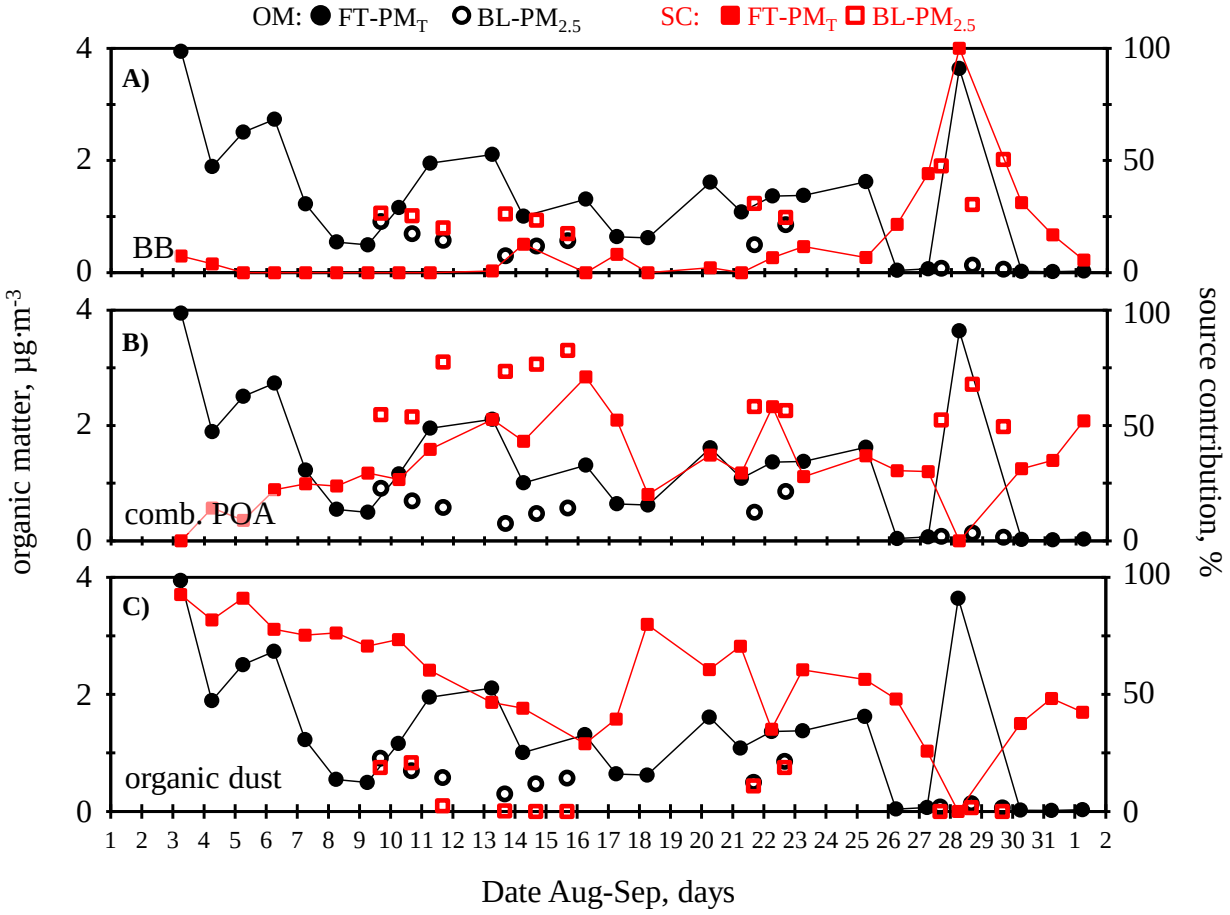

Figure 6: Time series of the total organic matter (OM; circle markers) and the source contribution (SC; square markers) to the determined organic matter for the FT-PM$_T$ (filled markets) and the BL-PM$_{2.5}$ samples (open markers). Sources: (**A**) biomass burning (BB), (**B**) combustion (comb.) POA and (**C**) organic dust.

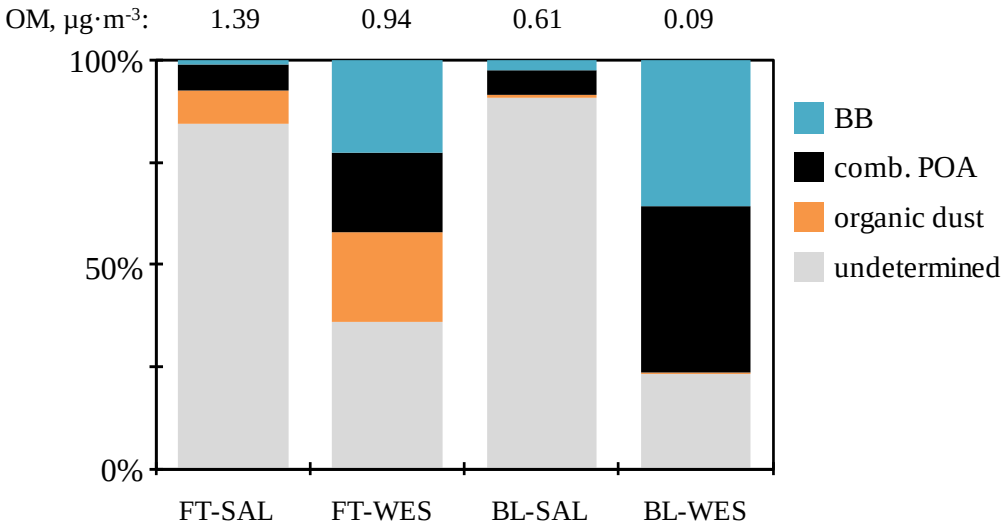

Figure 7: Contribution of the identified organic aerosol sources to the total organic matter within the FT and the BL under the SAL (FT-SAL and BL-SAL) and the WES (FT-WES, BL-WES, BBE). Average total OM for each air mass is on top. FT-PM_T samples were collected during the night (22–6 GMT) and BL-$PM_{2.5}$ samples were collected during the day (10–16 GMT).